EXPERIMENTAL DETERMINATION OF THE MOLECULAR DIFFUSION COEFFICIENT OF GASES BY ENHANCED DISPERSION IN OSCILLATORY FLOWS

By

GREGORY ALLEN ZACHRICH

A DISSERTATION PRESENTED TO THE GRADUATE SCHOOL
OF THE UNIVERSITY OF FLORIDA IN PARTIAL FULFILLMENT
OF THE REQUIREMENTS FOR THE DEGREE OF
DOCTOR OF PHILOSOPHY

UNIVERSITY OF FLORIDA

1995

ACKNOWLEDGEMENTS

Dr. Ulrich H. Kurzweg, chair of my committee, lead me through this research project. Although he performed many required tasks, specifically I thank him for reviewing this paper's various preliminary versions suggesting several modifications to improve the final copy. Also, his continued effort to keep me focused on the main topic of this dissertation is much appreciated.

Dr. E. Rune Lindgren, whom I consider a friend, prompted me to further my education. I thank him for allowing me to discuss many of my thoughts in confidence with him.

Dr. Marc Jaeger was extremely helpful in providing his laboratory equipment and assisting in the collection of data. Without his cooperation this work would not have been possible.

I thank the remainder of my committee, Drs. Shyy and Lear, for serving in their respective capacities as member and external member.

I truly appreciate the valued advice and guidance of Shirley Robinson, who, among other things, reminded me of the numerous deadlines that arose.

My mother, father, brothers and sister provided unquantifiable moral support during this long endeavor, for which I am most grateful.

TABLE OF CONTENTS

page

ACKNOWLEDGEMENTS.. ii

LIST OF TABLES.. vi

LIST OF FIGURES...vii

LIST OF SYMBOLS... ix

ABSTRACT..xii

CHAPTER 1 INTRODUCTION.................................... 1

CHAPTER 2 ESTIMATING THE DIFFUSION AND VISCOSITY COEFFICIENT IN GASES............................ 5
- Estimating the Diffusion Coefficient............. 5
- Estimating the Viscosity Coefficient............. 9

CHAPTER 3 ANALYTICAL SOLUTION FOR ENHANCED DISPERSION IN OSCILLATING FLOW.............................. 14
- Velocity Profile Solution........................ 14
- Concentration Solution........................... 23
- Determining the Enhanced Diffusion Coefficient... 26
- Tidal Displacement Solution...................... 32
- Enhanced Diffusion Coefficient in Final Form..... 38
- Graphical Presentation........................... 39

CHAPTER 4 EXPERIMENTAL PROCEDURE.......................... 41
- Enhanced Diffusion Process....................... 41
- Experimental Procedure........................... 44
- Experimental Assumptions......................... 48
  - Diffusion Coefficient is Independent of Concentration.............................. 48
  - Incompressible Gases........................ 49
  - Linear Concentration Gradient............... 50
  - Pressure Gradient is a Function of a Pure Sine Wave in Time.......................... 50
  - Cross-Sectional Velocity Profile is Fully Developed............................ 53
  - Transverse Diffusion Effects Overwhelms Axial Diffusion............................ 53
  - Flow is Completely Laminar.................. 54
  - Steady State Conditions have been Achieved.. 54
  - Tube is Completely Straight................. 55

All Measurements are Accurate.............. 55
No Leaks To or From Tube System............ 56
Tidal Displacement Remains Small........... 57
Deriving the Non-dimensional Expressions Used in the Experimental Measurements of the Two Setups.. 57
Determining Density and Viscosity Coefficients Experimentally................................ 63

CHAPTER 5 EXPERIMENTAL RESULTS........................ 64
Setup One.. 64
Setup Two.. 69
Pressure-Displacement............................ 73

CHAPTER 6 CONCLUSIONS................................ 75
Concluding Remarks............................... 75
Future Work...................................... 77

APPENDIX... 79

TABLE OF REFERENCES.................................. 84

BIOGRAPHICAL SKETCH.................................. 87

LIST OF TABLES

Table page

2.1 Tabulated Values of Parameters for Various Gases.............................. 8

2.2 Predicted and Reference Diffusion Coefficient 8

2.3 Predicted and Reference Viscosity........... 11

2.4 Diffusion Collision Integral................ 12

2.5 Viscosity Collision Integral................ 13

5.1 Raw Data Setup 1.......................... 67

5.2 Results Setup 1............................ 68

5.3 Raw Data Setup 2........................... 70

5.4 Results Setup 2............................ 71

5.5 Pressure-Displacement Results............... 74

TABLE OF FIGURES

Figure page

3.1 Plot of Log $J_0((-i)^{.5} x)$ 19

3.2 Plot of Log $J_1((-i)^{.5} x)$ 20

3.3 Plot of ber_0, bei_0, ber_1, and bei_1 21

3.4 Velocity Profiles at 0 Degree............... 22

3.5 Velocity Profiles at 30 Degree.............. 22

3.6 Velocity Profiles at 60 Degree.............. 22

3.7 Velocity Profiles at 90 Degree.............. 22

3.8 Velocity Profiles at 120 Degree............. 22

3.9 Velocity Profiles at 150 Degree............. 22

3.10 Pressure-Displacement Relationship (Smaller α)............................... 35

3.11 Pressure-Displacement Relationship (Larger α)................................ 36

3.12 Phase Between Pressure Gradient and Velocity 37

3.13 Contour Plot of $\lambda = D_{eff} / \omega \Delta x^2$ verses α and S 40

4.1 Schematic of Setup 1....................... 46

4.2 Schematic of Setup 2....................... 46

4.3 Photograph of Setup 2...................... 47

4.4 Photograph of Linear Motor Used to Produce Sinusoidal Axial Displacements of Fluid within Conduit............................ 50

4.5 Photograph of Pressure Variation and Tidal Volume.............................. 51

4.6 Contour Plot of $N(\alpha,S)$ 61
5.1 Experimental Data Setup 1 69
5.2 Experimental Data Setup 2 71
5.3 Experimental Data Pressure-Displacement Relationship 74

KEY TO SYMBOLS

α	Womersley Number, $\alpha = a \cdot (\omega \ / \ \nu)^{.5}$ (non-dimensional)
γ	Concentration Gradient (g/cm^4)
Δx	Tidal Displacement (cm)
ϵ	Intermolecular Distance (cm^{-8} = Å)
η	Radial Distance, $\eta = r/a$ (non-dimensional)
θ	Angular Direction (radian)
λ	Dispersion Function (non-dimensional)
μ	Dynamic Viscosity (g/cm s)
μ_{AIR}	Dynamic Viscosity of Air (1 cP = 0.01 g/cm s)
ν	Kinematic Viscosity (cm^2/s)
ρ	Density (g/cm^3)
$\Sigma \upsilon$	Atomic Diffusion Volume Increments
σ_{AB}	Intermolecular Distance (Å)
ω	Angular Frequency (1/s)
Ω_{μ}	Collision Integral for Viscosity
$\Omega_{D,AB}$	Collision Integral for Diffusion Coefficient
a	Radius of Tube (cm)
A	Cross-Sectional Area (cm^2)
c	Acoustic Velocity (cm/s)
C	Concentration (g/cm^3 or %)
D_{AB}	Molecular Diffusion Coefficient (cm^2/s)

D_{eff}	Effective Enhanced Diffusion (cm^2/s)
D_M	Molecular Diffusion Coefficient (cm^2/s)
dS	Circumferencial Distance $dS = \eta\ d\theta$ (non-dimensional)
$f(\eta)$	Non-dimensional Velocity Function
$F(\eta)$	Non-dimensional Concentration Function
$g(\eta)$	Non-dimensional Concentration Function
$G(\eta)$	Non-dimensional Concentration Function
$h(\eta)$	Non-dimensional Concentration Function
J_0	Bessel Function of First Kind of Zero Order
J_1	Bessel Function of First Kind of First Order
k_b	Boltzman's Constant (1.38054×10^{-23} J/molecule °K)
K	Magnitude of Pressure Grad. / density (Atm cm^2/g)
L	Length of Tube (cm)
M	Molecular weight (g/gmole)
N	Non-dimensional Function
P	Pressure (Atmospheres)
$\dot{Q}$	Volumetric Flow Rate (cm^3/s)
r	Radial Direction (cm)
R	Universal Gas Constant (8.3143 J/gmole °K)
S	Schmidt Number, $S = \nu / D_M$ (non-dimensional)
t	Time (s)
T	Temperature (°K)
T_c	Critical Temperature (°K)
u	Velocity (cm/s)
U_0	Mean Velocity (cm/s)
V	Volume of Isolation Chamber (cm^3)

V_c	Critical Specific Volume (m^3/Kg)
x	Axial Direction (cm)
Y_0	Bessel Function of Second Kind of Zero Order

Abstract of Dissertation Presented to the Graduate School
of the University of Florida in Partial Fulfillment of the
Requirements for the Degree of
Doctor of Philosophy

EXPERIMENTAL DETERMINATION OF THE MOLECULAR DIFFUSION COEFFICIENT OF GASES BY ENHANCED DISPERSION IN OSCILLATORY FLOW

by

Gregory Allen Zachrich

May 1995

Chairman: Ulrich H. Kurzweg
Major Department: Aerospace Engineering,
Mechanics, and
Engineering Sciences

This paper presents an experimental study of an alternative method to determine the molecular diffusion coefficient utilizing an enhanced axial dispersion process. Enhanced dispersion is a process by which a species in a fluid oscillating in a tube can experience a vastly amplified rate of effective diffusion as compared to normal molecular diffusion. This enhancement is promoted by an interaction between the boundary layer and the core within conduits as the fluid oscillates. The species is transferred first by diffusing radially into the boundary layer and later in the cycle diffusing, again radially, back into the oscillating core of the fluid, being transported axially a large distance from the originating location.

This enhanced dispersion process is completely described mathematically by a function dependent on the properties of the kinematic viscosity of the carrier fluid, the molecular diffusion coefficient of the diffusing species into the carrier fluid, the tube radius, the angular frequency of oscillation, and the axial tidal or bulk displacement.

Measurements of the diffusional flux were obtained with a sinusoidal frequency varying between 1.0 and 10.0 Hz, tidal displacement extending from 13.2 to 50.9 cm, and tube radius ranging from 0.19 to 1.03 cm in time-periodic steady state conditions. The experiment was conducted on two separate setups, one a system of multiple capillary tubes connecting two reservoirs with no net flow in the tubes, the other consisting of a single, larger tube between a reservoir and the atmosphere with a net flow. All measurements were made at room temperature (~300° K) and at one atmosphere pressure. Nine experimental runs were completed with nitrogen diffusing into oxygen and seven of oxygen diffusing into carbon dioxide. The experimental molecular diffusion coefficient was determined by a least sum-of-squares of error between the theoretical curve and the collected data. Also a predicted 'tuning effect' in this dispersion process was verified with optimum effective diffusion occurring in O_2-CO_2 mixtures near the Womersley number of 4.

The molecular diffusion coefficient of oxygen into carbon dioxide was determined to be 0.136 cm^2/s when reduced to 0° C and one atmosphere of pressure, compared to a tabulated value of 0.139 cm^2/s at the same conditions.

CHAPTER 1

INTRODUCTION

Diffusion is a process of mass transport due to the random molecular motion of the individual mass particles. Although Graham made experimental studies of the phenomena as early as 1803, the mathematical study of diffusion was first investigated by Fick in 1855. He found that diffusion was governed by the same mathematical expressions as Fourier had derived for heat conduction in 1822. Therefore, many solutions found for heat conduction are directly applicable to the diffusion processes (Crank 1975).

The study of diffusion in gases was first recorded in 1870 when Loschmidt devised a method to experimentally determine the diffusion coefficient. His apparatus consisted of two cylinders placed vertically, separated by a stopcock. Into this device were placed the two gases that were to be studied. The more dense gas was placed in the lower chamber to preclude the likelihood of convective currents internally, causing mixing that would artificially, but erroneously, increase the determined numeric diffusion coefficient. Once the experiment was prepared, the stopcock was opened, and after a predetermined time was closed. After the experiment was concluded, the chemical composition of the two chambers were determined, usually by chemical adsorption of one of the gases, which provided the raw data to determine the diffusion coefficient.

In 1907 an improvement to the original method, a sliding disk that had the full cylinder diameter available for the diffusion was implemented. This allowed for a greater rate of diffusion, due to the increased area, which increased the accuracy of the measurement. In this apparatus, temperature, pressure and concentration dependance were investigated.

It was determined that the temperature dependance went at $T^{1.5}$ power. The pressure dependance was found to be inversely proportional to the pressure, and the concentration dependance was generally very limited, but nearly the square root of the molecular weight of the gas mixture.

The study of accelerated diffusion in pipe flow was investigated by Taylor (1958), who studied both laminar and turbulent steady flow conditions. As an experimental verification of his theory, he injected salt into flowing water and obtained a diffusion distribution some distance downstream. This study invalidated earlier assumptions that the salt would flow as a 'block' downstream, and proved that there was an interaction between the boundary layer and the core flow. Taylor (1953) showed mathematically that the apparent dispersion coefficient could be written as

$K = \frac{U^2 a^2}{48 D_M}$, where U is the mean flow velocity, a is the tube radius, and D_M is the molecular diffusion coefficient.

Aris in 1956 showed that Taylor, by neglecting the axial diffusion in the derivation of his equation, had to place many restrictions on the applicability of his result. A more precise statement is that the axial molecular diffusion rate remained in the equation as $K = D_M + \frac{U^2 a^2}{48 D_M}$. This eliminated all of the restrictions of Taylor (Aris, 1956).

Taylor also showed that the molecular diffusion coefficient can be determined by measuring the spread caused by this enhanced diffusion method (Taylor, 1953). Since that time, the measurement of the diffusion coefficient has been improved through a method of streaming diffusion, which is essentially identical to the method described by Taylor. This method uses a technique of injecting a small amount of fluid into a laminar flow of a carrier fluid. The smaller quantity is dispersed throughout the carrier fluid by the action of radial diffusion. This spread can then be used to determine the molecular diffusion of the generally smaller quantity into the generally larger quantity carrier fluid. The advantage in this method is the amplification factor that is achieved by this spreading action. This method is now generally called the 'point source' method for determining molecular diffusion coefficient.

Harris and Goren (1967) first examined axial dispersion in capillaries under pure oscillatory conditions. This was followed by Watson studying this oscillatory diffusion in much greater detail in 1982. Watson derived the generalized equations for enhanced axial dispersion for any given tube cross-section and also with superimposed steady net flow.

Various papers have been written on the subject of enhanced diffusion by oscillatory motion (Dreyer et al. 1968) (Joshi, et al., 1983) (Jaeger and Kurzweg, 1983) (Kurzweg and Jaeger, 1986, 1987) (Jaeger et al. 1991) (Jaeger and Kalle, 1992). These papers generally proved experimentally that the theory was in good agreement with experimental data.

Because of the practical limitation of experimentally obtaining diffusion coefficients for all conditions and all possible combinations of components, a method was needed to reliably estimate the diffusion coefficient. This was attempted by Chen, Othermer and others starting in the early 1960s.

CHAPTER 2

ESTIMATING THE DIFFUSION AND VISCOSITY COEFFICIENT IN GASES

The actual documented data on molecular diffusion is quite limited. It is rather unlikely that the actual conditions required for a specific request of a molecular diffusion coefficient has experimentally been determined. Because of this, much work has been performed on devising a method to estimate the diffusion coefficient for any given components, temperature and pressure.

Estimating the Diffusion Coefficient

Most of the methods for estimating the diffusion coefficient require the use of tables of self-diffusion. These tables are based on identical and undistinguishable components diffusing into one another. These tables are normally generated by using isotopes of the various gases to closely approximate the identical and undistinguishable requirement. From these test runs, several parameters are calculated such as the collision diameter, an intermolecular characteristic distance, and a collision integral. Kinetic gas theory and quantum mechanics provide these parameters which may subsequently be used to estimate the diffusion of one substance into another substance.

Reid and Sherwood (1966) recommended using the following equation as an estimator of the molecular diffusion coefficient.

$$D_{AB}=\frac{0.0018583T^{3/2}}{P(\sigma_{AB})^2\Omega_{D,AB}}\sqrt{\frac{1}{M_A}+\frac{1}{M_B}} \tag{2.1}$$

In this equation T is the temperature in degrees Kelvin, P is the pressure in Atmospheres, and σ_{AB} is the molecular diameter in Angstroms, which is determined from quantum mechanics and is tabulated for various gases. The collision integral, $\Omega_{D,AB}$, is determined from a tabulation (Table 2.4) of the temperature forming a non-dimensional term k_BT/ϵ_{AB} where k_B is Boltzman's constant, the Lennard-Jones force constant, ϵ_{AB}, is estimated as $\epsilon_{AB}=\sqrt{\epsilon_a\epsilon_B}$ and σ_{AM} is estimated as $\sigma_{AB}=\frac{1}{2}(\sigma_A+\sigma_B)$. Again ϵ_A, ϵ_B, σ_A, and σ_B are tabulated for the various gases. The molecular weights of the gases are M_A and M_B. For equation 2.1 the average error for 114 measured values of diffusion coefficient in 65 binary systems at various temperatures was 7.5% (Skelland 1974).

Also, Fuller, Schettler, and Giddings (1966) suggested using the equation

$$D_{AB}=\frac{0.00100T^{7/4}}{P[(\Sigma v)_A^{1/3}+(\Sigma v)_B^{1/3}]^2}\sqrt{\frac{1}{M_A}+\frac{1}{M_B}} \quad . \tag{2.2}$$

Here Σv is the sum of V_i which are tabulated Atomic Diffusion Volume Increments. This equation has an average error of 6.9% for 114 measured values of 65 binary systems (Skelland 1974).

Chen and Othmer (1962) suggested the version,

$$D_{AB}=\frac{0.0150T^{1.81}}{P(T_{cA}T_{cB})^{0.1405}(V_{cA}^{0.4}+V_{cB}^{0.4})^2}\sqrt{\frac{1}{M_A}+\frac{1}{M_B}} \quad , \tag{2.3}$$

where P is in atmospheres, T_c the critical temperature in degrees Kelvin, V_c the critical specific volume in cubic centimeters per gram-mole. This equation has an average error of 8.5% for 114 measured values of 65 binary systems at various temperature (Skelland 1974).

Othmer and Chen (1962) suggested the equation

$$D_{AB}=(2.52x10^7)\mu_{air}^{2.74}\left[\frac{\sqrt{\frac{1}{M_A}+\frac{1}{M_b}}}{(V_{cA}^{0.4}+V_{cB}^{0.4})^2}\right]^{1.23} \quad . \tag{2.4}$$

Here μ_{air} is the dynamic viscosity measured in cP (CentiPoise), where $1\,cP=0.01\,g/(cm\cdot s)$, at the temperature and pressure of the system in question. This equation has an average error of 12.6% for the same measured values (Skelland 1974).

At room temperature (300° K) and one atmosphere of pressure, the tabulated values are shown in Table 2.1.

Table 2.1 Tabulated Values of Parameters for Various Gases

Gas	ν $\frac{cm^2}{s}$	ρ $\frac{kg}{m^3}$	σ m^{-10}	ϵ/k $°K$	V_i	T_c $°K$	V_c cm^3/g
Air	0.1566	1.177	3.711	78.6	20.1	132.4	2.857
CO_2	0.085	1.788	3.941	195.2	26.9	304.2	2.174
He	1.240	0.1624	2.551	10.22	2.88	5.25	14.43
N_2	0.1553	1.138	3.798	71.4	17.9	126.1	3.215
O_2	0.1585	1.299	3.467	106.7	16.6	154.4	2.326

ν,ρ (Edwards et al.) $\sigma,\epsilon/k,V_i$ (Skelland) T_c,V_c (Perry & Chilton)

At 300°K and one Atmosphere, the following table provides the calculated estimates for various combinations of gases.

Table 2.2 Predicted and Reference Diffusion Coefficient

Gas	Eq 2.1 cm^2/s	Eq 2.2 cm^2/s	Eq 2.3 cm^2/s	Eq 2.4 cm^2/s	Adjusted Table cm^2/s	Original Table cm^2/s
He->CO_2	0.828	0.801	1.063	1.03		
O_2->CO_2	0.154	0.163	0.168	0.171	0.164	0.139
N_2->O_2	0.208	0.210	0.217	0.201	0.213	0.181

Reference values (Hirschfelder, et al. 1949)

The table reference has been adjusted to 300 degree Kelvin from 0 degree Centigrade by the 7/4 power rule. (Chapman & Cowling 1953)

Estimating the Viscosity Coefficient

The dynamic viscosity of a low density gas can be predicted by the equation

$$\mu = 2.6693 x 10^{-5} \frac{\sqrt{MT}}{\sigma^2 \Omega_\mu} \quad , \tag{2.5}$$

where μ is in $g/(cm \cdot \text{sec})$, M is the Molecular Weight of the gas, T is the Temperature in degrees Kelvin, σ is in angstroms, which is a tabulated value, and Ω_μ is also a tabulated value (Table 2.5) determined from $\frac{kT}{\epsilon}$ as in the diffusion coefficient prediction equations, but of a different value (Bird, et al. 1960).

The National Bureau of Standards have produced formulas for predicting the dynamic viscosity of several gases. These are simply interpolation formulas from a best fit quadratic curve in both temperature and pressure to tabulated data.

$$\begin{gathered}\mu_{air} = 170.256 + 0.605434\,T \\ - 0.001332\,T^2 + 1.17237\,P \\ + 0.125639\,P^2\end{gathered} \tag{2.6}$$

$$\begin{gathered}\mu_{N_2} = 167.214 + 0.392728\,T \\ + .00122474\,T^2 + 1.24165\,P \\ + 0.0987206\,P^2\end{gathered} \tag{2.7}$$

$$\mu_{CO_2} = 137.339 + 0.441133\,T + .00112987\,T^2 + 0.0628105\,P + 0.562974\,P^2 \tag{2.8}$$

$$\mu_{O_2} = 190.395 + 0.650043\,T - .000897542\,T^2 + 0.130897\,P + .00132418\,P^2 \tag{2.9}$$

in which μ is in $\mu g/(cm \cdot s)$, T is in °C and P is in atmospheres (Jones, 1984).

Chapman and Enskog developed the following equation to predict the viscosity of multi-component system

$$\mu_{mix} = \sum_{i=1}^{n} \frac{x_i\, u_i}{\sum_{j=1}^{n} x_j\, \Phi_{ij}} \tag{2.10}$$

in which

$$\Phi_{ij} = \frac{\left[1 + \left(\frac{\mu_i}{\mu_j}\right)^{1/2} \left(\frac{M_j}{M_i}\right)^{1/4}\right]^2}{\sqrt{8}\left(1 + \frac{M_i}{M_j}\right)^{1/2}} \quad . \tag{2.11}$$

Here n is the total number of species, x_i and x_j are the mole fractions of the species i and j. μ_i and μ_j are the dynamic viscosities at the pressure and temperature of the system, and M_i and M_j are the molecular weights of the species. This equation has been shown to produce results within 2% of μ_{mix} values (Bird, et al. 1960).

The kinematic viscosity can be calculated from $\nu=\frac{\mu}{\rho}$, where for conditions sufficiently far removed from the critical point, and from phase transitions, the equation of state $\rho=\frac{P}{RT}$ may be used.

Table 2.3 Predicted and Reference Viscosity

Gas	$\mu_{eq2.5}$ $\frac{10^{-4}g}{cm\cdot sec}$	$\rho=\frac{P}{RT}$ $\frac{kg}{m^3}$	$\nu_{eq2.5}$ $\frac{cm^2}{sec}$	μ_{ref} $\frac{10^{-4}g}{cm\cdot sec}$	ρ_{ref} $\frac{kg}{m^3}$	ν_{ref} $\frac{cm^2}{sec}$
Air	1.837	1.172	0.1567	1.843	1.177	0.1566
CO_2	1.524	1.789	0.0852	1.520	1.788	0.085
O_2	2.057	1.301	0.1581	2.059	1.299	0.1585
N_2	1.767	1.139	0.1551	1.767	1.138	0.1553

ρ_{ref} (Edwards et at.) ν_{ref} (Johnson, McCloskey) $\mu_{ref}=\rho_{ref}\nu_{ref}$

Table 2.4 Diffusion Collision Integral (Skelland 1974)

kT/ϵ	Ω_D	kT/ϵ	Ω_D	kT/ϵ	Ω_D
0.30	2.662	1.65	1.153	4.0	0.8836
0.35	2.476	1.70	1.140	4.1	0.8788
0.40	2.318	1.75	1.128	4.2	0.8740
0.45	2.184	1.80	1.116	4.3	0.8694
0.50	2.066	1.85	1.105	4.4	0.8652
0.55	1.966	1.90	1.094	4.5	0.8610
0.60	1.877	1.95	1.084	4.6	0.8568
0.65	1.798	2.00	1.075	4.7	0.8530
0.70	1.729	2.1	1.057	4.8	0.8492
0.75	1.667	2.2	1.041	4.9	0.8456
0.80	1.612	2.3	1.026	5.0	0.8422
0.85	1.562	2.4	1.012	6	0.8124
0.90	1.517	2.5	0.9996	7	0.7896
0.95	1.476	2.6	0.9878	8	0.7712
1.00	1.439	2.7	0.9770	9	0.7556
1.05	1.406	2.8	0.9672	10	0.7424
1.10	1.375	2.9	0.9576	20	0.6640
1.15	1.346	3.0	0.9490	30	0.6232
1.20	1.320	3.1	0.9406	40	0.5960
1.25	1.296	3.2	0.9328	50	0.5756
1.30	1.273	3.3	0.9256	60	0.5596
1.35	1.253	3.4	0.9186	70	0.5464
1.40	1.233	3.5	0.9120	80	0.5352
1.45	1.215	3.6	0.9058	90	0.5256
1.50	1.198	3.7	0.8998	100	0.5170
1.55	1.182	3.8	0.8942	200	0.4644
1.60	1.167	3.9	0.8888	400	0.4170

Table 2.5 Viscosity Collision Integral (Bird, et al. 1960)

kT/ϵ	Ω_μ	kT/ϵ	Ω_μ	kT/ϵ	Ω_μ
0.30	2.785	1.65	1.264	4.0	0.9700
0.35	2.628	1.70	1.248	4.1	0.9649
0.40	2.492	1.75	1.234	4.2	0.9600
0.45	2.368	1.80	1.221	4.3	0.9553
0.50	2.257	1.85	1.209	4.4	0.9507
0.55	2.156	1.90	1.197	4.5	0.9464
0.60	2.065	1.95	1.186	4.6	0.9422
0.65	1.982	2.00	1.175	4.7	0.9382
0.70	1.908	2.1	1.156	4.8	0.9343
0.75	1.841	2.2	1.138	4.9	0.9305
0.80	1.780	2.3	1.122	5.0	0.9269
0.85	1.725	2.4	1.107	6	0.8963
0.90	1.675	2.5	1.093	7	0.8727
0.95	1.629	2.6	1.081	8	0.8538
1.00	1.587	2.7	1.069	9	0.8379
1.05	1.549	2.8	1.058	10	0.8242
1.10	1.514	2.9	1.048	20	0.7432
1.15	1.482	3.0	1.039	30	0.7005
1.20	1.452	3.1	1.030	40	0.6718
1.25	1.424	3.2	1.022	50	0.6504
1.30	1.399	3.3	1.014	60	0.6335
1.35	1.375	3.4	1.007	70	0.6194
1.40	1.353	3.5	0.9999	80	0.6076
1.45	1.333	3.6	0.9932	90	0.5973
1.50	1.314	3.7	0.9870	100	0.5882
1.55	1.296	3.8	0.9811	200	
1.60	1.279	3.9	0.9755	400	

CHAPTER 3

ANALYTICAL SOLUTION FOR ENHANCED DISPERSION IN OSCILLATING FLOW

The molecular diffusion coefficient and kinematic viscosity are two properties that will arise in connection with the analytical solution to the enhanced axial dispersion in tubes to be developed next. Their values will be directly determined from the relation to be devised below.

Velocity Profile Solution

Oscillating flow of a fluid with a axial concentration gradient is controlled by both the Navier-Stokes Equation and Fick's Law. The Navier-Stokes Equations control the physical flow of the fluid as a whole, while Fick's Law controls the diffusion within this fluid.

The Navier-Stokes equation for an incompressible fluid is

$$\frac{D\vec{u}}{Dt} = -\frac{1}{\rho}\vec{\nabla}P + \nu\,\nabla^2\vec{u} \qquad (3.1)$$

where $\frac{D}{Dt}$ is the material derivative, $\vec{\nabla}$ is the gradient operator, and ∇^2 is the Laplacian operator. In cylindrical coordinates the Navier-Stokes equation reads

$$\begin{gathered}\frac{\partial \vec{u}}{\partial t} + (u_r \cdot \frac{\partial}{\partial r})\,\vec{u} + (u_\theta \cdot \frac{\partial}{\partial \theta})\,\vec{u} + (u_x \cdot \frac{\partial}{\partial x})\,\vec{u} = \\ -\frac{1}{\rho}\frac{\partial P}{\partial \vec{x}} + \nu\left[\frac{1}{r}\left\{\frac{\partial}{\partial r}\left(r\,\frac{\partial}{\partial r}\right) + \frac{\partial}{\partial \theta}\left(\frac{1}{r}\frac{\partial}{\partial \theta}\right) + \frac{\partial}{\partial x}\left(r\frac{\partial}{\partial x}\right)\right\}\right]\vec{u}\end{gathered} \quad , \qquad (3.2)$$

where the velocity $\vec{u} = e_r u_r + e_\theta u_\theta + e_x u_x$ and e_r, e_θ, e_x are unit base vectors in the radial, angular, and axial direction, respectively. For pure oscillating flow confined to a tube of infinite length and circular cross section, the fluid velocity is independent of angular direction and axial location. These assumptions reduce the Navier-Stokes equation to

$$\frac{\partial u}{\partial t} = -\frac{1}{\rho}\frac{\partial P}{\partial x} + \nu\left(\frac{\partial^2 u}{\partial r^2} + \frac{1}{r}\frac{\partial u}{\partial r}\right) \quad . \qquad (3.3)$$

Here, $u = u_x$ is the velocity in the x direction along the length of the pipe. If it is assumed that the pressure gradient varies periodically in time as

$$-\frac{1}{\rho}\frac{\partial P}{\partial x} = K e^{i\omega t} \qquad (3.4)$$

where $K = \left|\frac{1}{\rho}\frac{\partial P}{\partial X}\right|$ is a constant and a measure of the magnitude of the pressure gradient, and the velocity is taken to vary as

$$u(\eta, t) = \Re\left[U_0 f(\eta) e^{i\omega t}\right] , \qquad (3.5)$$

where $\eta = \frac{r}{a}$ is a non-dimensional radius. With these assumptions, equation 3.3 becomes

$$\frac{i\omega}{\nu} f = \frac{K}{U_0 \nu} + \nabla^2 f \qquad (3.6)$$

or

$$\frac{\partial^2 f}{\partial \eta^2} + \frac{1}{\eta}\frac{\partial f}{\partial \eta} - \frac{i\omega a^2}{\nu} f = -\frac{K a^2}{U_0 \nu} \quad . \qquad (3.7)$$

An analytical solution can be found for this equation using the appropriate boundary conditions of $f(0)$ = *finite* and $f(1) = 0$ (no slip condition) (Schlichting 1960).

The solution of equation (3.7) is

$$f(\eta) = A\, J_0\left(\eta\sqrt{\frac{-i\,\omega\, a^2}{\nu}}\right) + B\, Y_0\left(\eta\sqrt{\frac{-i\,\omega\, a^2}{\nu}}\right) - i\,\frac{K}{U_0\,\omega} \quad . \tag{3.8}$$

Introducing the non-dimensional Womersley Number $\alpha = a\sqrt{\frac{\omega}{\nu}}$

and applying the above boundary conditions, one finds

$$f(\eta) = \frac{-i\,K}{U_0\,\omega}\left(1 - \frac{J_0(\sqrt{-i}\alpha\eta)}{J_0(\sqrt{-i}\alpha)}\right) \tag{3.9}$$

or since $u(\eta,t) = \Re\left[U_0\, f(\eta)\, e^{i\omega t}\right]$, that

$$u(\eta,t) = \Re\left[-i\frac{K}{\omega}e^{i\omega t}\left(1 - \frac{J_0(\sqrt{-i}\,\alpha\eta)}{J_0(\sqrt{-i}\,\alpha)}\right)\right] \quad . \tag{3.10}$$

Generally, $J_n(\sqrt{-i}x)$ can also be written as the Kelvin functions $ber_n(x) + i\; bei_n(x)$ where $ber_n(x)$ is the real portion of the function and $bei_n(x)$ is the imaginary part. One can then rewrite equation (3.9) and (3.10) as

$$f(\eta) = \frac{-i\,K}{U_0\,\omega}\left(1 - \frac{ber_0(\alpha\eta) + i\,bei_0(\alpha\eta)}{ber_0(\alpha) + i\,bei_0(\alpha)}\right) \tag{3.11}$$

so that

$$u(\eta, t) = \Re\left[-i\frac{K}{\omega}e^{i\omega t}\left(1 - \frac{ber_0(\alpha\eta) + i\ bei_0(\alpha\eta)}{ber_0(\alpha) + i\ bei_0(\alpha)}\right)\right] \quad . \tag{3.12}$$

Figures 3.1 and 3.2 show log plots of $J_0(\sqrt{-i}\,x)$ and $J_1(\sqrt{-i}\,x)$ which have a general shape of a spiral. The functions deviate from the spiral shape only when the independent variable is below a value of about x = 5. This prediction of the Kelvin functions has heretofore not been observed, but follows directly from the asymptotic form of $ber_n(x)$ and $bei_n(x)$ as given in Abramowitz and Stegan (1972). For large x one finds

$$ber_0(x) + i\,bei_0(x) \approx \frac{e^{x\sqrt{i}}}{\sqrt{2\pi x}} \tag{3.13}$$

Figure 3.1 Plot of Log $J_0((-i)^{.5} x)$

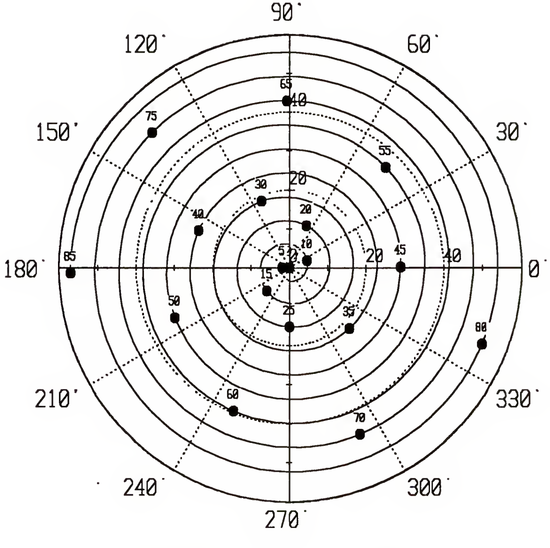

(Numbered Points are values of x)

Figure 3.2 Plot of Log $J_1((-i)^{.5} x)$

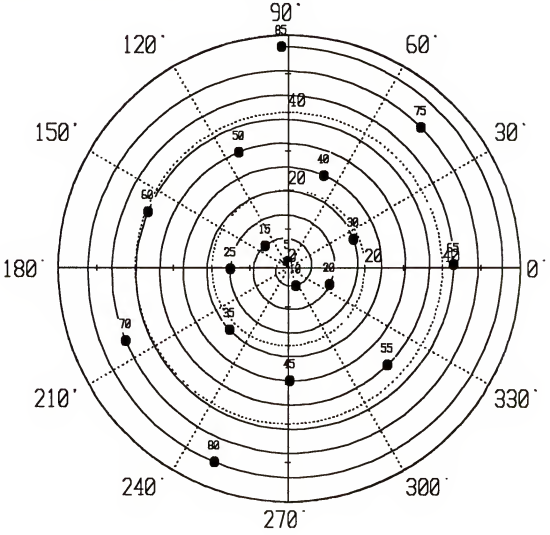

(Numbered Points are values of x)

Figure 3.3 has the various Kelvin functions plotted for the independent variable from zero to six. This is the range of variables where figures 3.1 and 3.2 deviate from the spiral shape.

Figure 3.3 Plot of ber_0, bei_0, ber_1, and bei_1

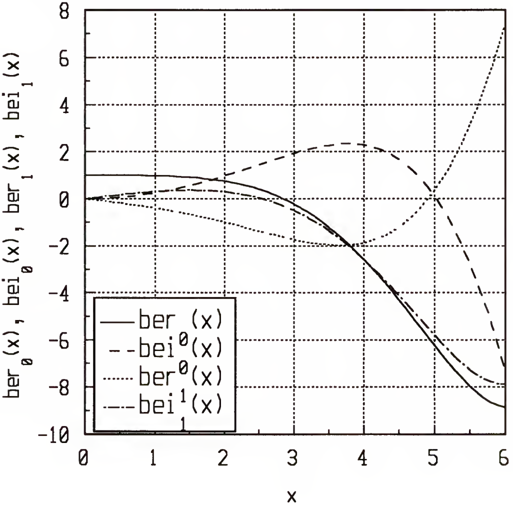

Figures 3.4 through 3.9 are velocity profiles given by equation 3.12 at various specified phases of the pressure gradient. Note that the boundary layer thickness is reduced at higher Womersley Numbers.

Figure 3.4 Velocity Profile at 0 Degree

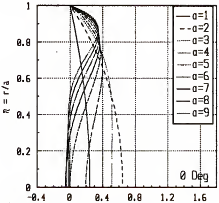

Figure 3.5 Velocity Profile at 30 Degree

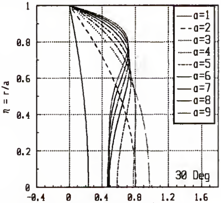

Figure 3.6 Velocity Profile at 60 Degree

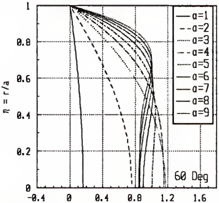

Figure 3.7 Velocity Profile at 90 Degree

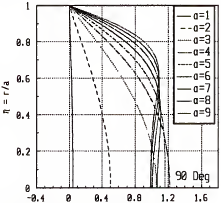

Figure 3.8 Velocity Profiles at 120 Degree

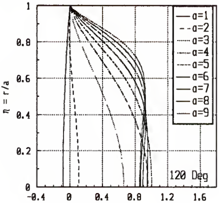

Figure 3.9 Velocity Profile at 150 Degree

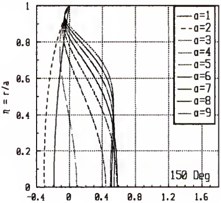

Velocity Profiles at Specified Pressure Phase for Various Womersley Numbers

Concentration Solution

Using this velocity profile in Fick's Equation for diffusion

$$\frac{\partial C}{\partial t} + \left(u\frac{\partial}{\partial x}\right) C = D_M \nabla^2 C \tag{3.14}$$

and making the approximation for concentration of

$$C(\eta, x, t) = \gamma \left(x + E g(\eta) e^{i\omega t}\right) \tag{3.15}$$

which was introduced by Chatwin (1975), equation 3.14 becomes

$$\frac{i\omega}{D_M} g + \frac{U_0}{D_M E} f = \nabla^2 g \tag{3.16}$$

or

$$\frac{\partial^2 g}{\partial \eta^2} + \frac{1}{\eta}\frac{\partial g}{\partial \eta} - \frac{i\omega a^2}{D_M} g = \frac{a^2 U_0}{D_M E} f \quad . \tag{3.17}$$

Note that $\frac{\omega a^2}{D_M}$ can be re-written as $\frac{\omega a^2}{\nu}\frac{\nu}{D_M} = \alpha^2 S$ where S is the Schmidt number, so that one has the alternate form

$$\frac{\partial^2 g}{\partial \eta^2} + \frac{1}{\eta}\frac{\partial g}{\partial \eta} - i\alpha^2 S g = \frac{a^2 U_0}{D_M E} f \quad . \tag{3.18}$$

This equation is subject to the boundary conditions $\frac{\partial g(1)}{\partial \eta} = 0$ (no diffusion through the wall) and $g(0) = finite$. Assuming a solution of the form

$$g(\eta) = (f(\eta) + h(\eta))F \quad , \tag{3.19}$$

equation 3.18 becomes

$$\frac{\partial(f+h)}{\partial \eta^2} + \frac{1}{\eta}\frac{\partial(f+h)}{\partial \eta} - i\alpha^2 S(f+h) = \frac{a^2 U_0}{D_M E F} f \quad . \tag{3.20}$$

Using equation (3.7), the partial's of f can be eliminated resulting in

$$\frac{\partial^2 h}{\partial \eta^2} + \frac{1}{\eta}\frac{\partial h}{\partial \eta} - i\,\alpha^2 S h = \left(\frac{a^2 U_0}{D_M E F} + i\,\alpha^2\,(S-1)\right) f + \frac{K a^2}{U_0 \nu} \quad . \tag{3.21}$$

Setting $F = i\frac{U_0 S}{E\omega\,(S-1)}$, the f term drops out leaving us with the equation

$$\frac{\partial^2 h}{\partial \eta} + \frac{1}{\eta}\frac{\partial h}{\partial \eta} - i\alpha^2 S h = \frac{K a^2}{U_0 \nu} \quad . \tag{3.22}$$

The solution to this equation is

$$h(\eta) = G J_0(\sqrt{-iS}\,\alpha\,\eta) + H Y_0(\sqrt{-iS}\,\alpha\,\eta) + i\frac{K}{U_0\,\omega\,S} \quad . \qquad (3.23)$$

To satisfy $g(0)$ = *finite* the parameter H must equal zero. Also from the Bessel function derivative identity $\frac{\partial J_0(x)}{\partial x} = -J_1(x)$, we have

$$\frac{\partial J_0(\sqrt{-iS}\,\alpha\eta)}{\partial\eta} = -\sqrt{-iS}\,\alpha\;J_1(\sqrt{-iS}\,\alpha\eta) \quad . \qquad (3.24)$$

The derivative for $g(\eta)$ is

$$\left.\frac{\partial g(\eta)}{\partial\eta}\right|_{\eta=1} = 0 =$$

$$i\frac{U_0\,S}{E\,\omega\,(S-1)}\left(-G\sqrt{-iS}\,\alpha\,J_1(\sqrt{-iS}\,\alpha) - i\frac{K\sqrt{-i}\,\alpha}{U_0\,\omega}\,\frac{J_1(\sqrt{-i}\,\alpha)}{J_0(\sqrt{-i}\,\alpha)}\right) \quad . \qquad (3.25)$$

Solving for G, one finds

$$G = -i\frac{K J_1(\sqrt{-i}\,\alpha)}{U_0\,\omega\,\sqrt{S}\;J_0(\sqrt{-i}\,\alpha)\,J_1(\sqrt{-iS}\,\alpha)} \quad . \qquad (3.26)$$

Therefore

$$g(\eta) =$$

$$\frac{K}{E\omega^2 (S-1)} \left(\frac{\sqrt{S}\, J_1(\sqrt{-i}\,\alpha)\, J_0(\sqrt{-iS}\,\alpha\,\eta)}{J_0(\sqrt{-i}\,\alpha)\, J_1(\sqrt{-iS}\,\alpha)} - \frac{S\, J_0(\sqrt{-i}\,\alpha\,\eta)}{J_0(\sqrt{-i}\,\alpha)} + S - 1 \right) \tag{3.27}$$

Determining the Enhanced Diffusion Coefficient

The enhanced coefficient of diffusion for oscillatory flow can be determined by setting the effective diffusion equal to the time averaged net concentration flux through the cross-sectional area, of the tube. Mathematically one has

$$D_{eff}\, A \frac{\partial C}{\partial x} = \int u\, C\, dA \tag{3.28}$$

In this integral, $u = U_0 (u_R + i\, u_I)$, where $u_R = \dfrac{f e^{i\omega t} + \bar{f} e^{-i\omega t}}{2}$

and $u_I = \dfrac{f e^{i\omega t} - \bar{f} e^{-i\omega t}}{2}$, and $C = C_R + i\, C_I$, where

$C_R = \gamma \left(z + \dfrac{E g e^{i\omega t} + E \bar{g} e^{-i\omega t}}{2} \right)$ and $C_I = E\gamma \dfrac{g e^{i\omega t} - \bar{g} e^{-i\omega t}}{2}$.

The bar denotes the complex conjugate of the function and R and I refer to the Real and Imaginary components respectively. Equation (3.28) may thus be re-written as

$$D_{eff} A \frac{\partial C}{\partial x} = U_0 \int \left(\frac{f e^{i\omega t} + \overline{f} e^{-i\omega t}}{2} + i \, \frac{f e^{i\omega t} - \overline{f} e^{-i\omega t}}{2} \right) \gamma \left[\left(z + \frac{E g e^{i\omega t} + E \overline{g} e^{-i\omega t}}{2} \right) + i \, \frac{E g e^{i\omega t} - E \overline{g} e^{-i\omega t}}{2} \right] dA \tag{3.29}$$

or

$$D_{eff} A \frac{\partial C}{\partial z} = U_0 \gamma \int \left(\frac{(1+i)}{2} f e^{i\omega t} + \frac{(1-i)}{2} \overline{f} e^{-i\omega t} \right) \left(z + \frac{(1+i)}{2} E g e^{i\omega t} + \frac{(1-i)}{2} E \overline{g} e^{-i\omega t} \right) dA \quad . \tag{3.30}$$

When integrated over the one period of oscillation to obtain a time averaged value, the remaining terms will be time independent. The resulting time averaged integral reads

$$D_{eff} A \frac{\partial C}{\partial x} = \frac{E U_o \gamma}{2} \int \left(f(\eta) \overline{g}(\eta) + \overline{f}(\eta) g(\eta) \right) dA \tag{3.31}$$

The application of Green's Theorem will transform this last integral into a form that is more easily solved. When equation (3.6) is multiplied by the conjugate of g and the conjugate of equation (3.16) is multiplied by f, one finds

$$\frac{i\,\omega}{\nu}\, f\,\overline{g} = \frac{K}{U_0\,\nu}\,\overline{g} + \overline{g}\,\nabla^2 f \qquad (3.32)$$

and

$$-\frac{i\,\omega}{\nu}\, f\,\overline{g} + \frac{U_0}{D\,E} f\,\overline{f} = f\,\nabla^2\overline{g} \quad . \qquad (3.33)$$

When (3.33) is subtracted from (3.32), one has

$$\left(\frac{i\,\omega}{D_M} + \frac{i\,\omega}{\nu}\right) f\,\overline{g} - \frac{U_0}{D_M E}\, f\,\overline{f} = \frac{K}{\nu\, U_0}\,\overline{g} + \overline{g}\,\nabla^2 f - f\,\nabla^2\overline{g} \quad . \qquad (3.34)$$

It is desirable to eliminate $\overline{g}$ from this equation. This can be done by inserting into equation (3.16) the equivalent of f from equation (3.6), taking the conjugate of the result. That is,

$$\overline{g} = \frac{K\,U_0}{\omega^2\,E} + \frac{\nu\, U_0}{\omega^2\,E}\nabla^2\overline{f} + \frac{i\,D_M}{\omega}\nabla^2\overline{g} \quad . \qquad (3.35)$$

This yields

$$\overline{g}\nabla^2 f - f\nabla^2\overline{g} + \frac{i\,KD_M}{\omega\,\nu\,U_0}\nabla^2\overline{g} + \frac{K}{\omega^2\,E}\nabla^2\overline{f} = \left(\frac{i\,\omega}{\nu} + \frac{i\omega}{D_M}\right) f\,\overline{g} - \frac{U_0}{D_M E} f\,\overline{f} - \frac{K^2}{\nu\,\omega^2\,E} \tag{3.36}$$

and the conjugate of the above is

$$g\nabla^2\overline{f} - \overline{f}\nabla^2 g - \frac{i\,KD_M}{\omega\,\nu\,U_0}\nabla^2 g + \frac{K}{\omega^2\,E}\nabla^2 f = -\left(\frac{i\,\omega}{\nu} + \frac{i\omega}{D_M}\right)\overline{f}\,g - \frac{U_0}{D_M E}\overline{f}\,f - \frac{K^2}{\nu\,\omega^2\,E} \;. \tag{3.37}$$

Now (3.37) is subtracted from (3.36) which gives

$$\overline{g}\nabla^2 f - g\nabla^2\overline{f} - f\nabla^2\overline{g} + \overline{f}\nabla^2 g + \frac{i\,KD_M}{\omega\,\nu\,U_0}\left(\nabla^2\overline{g} + \nabla^2 g\right) + \frac{K}{\omega^2\,E}\left(\nabla^2\overline{f} - \nabla^2 f\right) = \left(\frac{i\,\omega}{\nu} + \frac{i\,\omega}{D_M}\right)\left(f\,\overline{g} + \overline{f}\,g\right) \;. \tag{3.38}$$

Equation 3.38 is inserted into equation 3.31 which yields

$$D_{eff} A \frac{\partial C}{\partial z} = \frac{U_0 D_M S E}{i \omega (S+1)} \frac{\gamma}{2} \cdot$$

$$\int \left(\overline{g} \nabla^2 f - g \nabla^2 \overline{f} - f \nabla^2 \overline{g} + \overline{f} \nabla^2 g + \frac{i K D_M}{\omega \nu U_0} (\nabla^2 \overline{g} + \nabla^2 g) + \frac{K}{\omega^2 E} (\nabla^2 \overline{f} - \nabla^2 f) \right) dA \tag{3.39}$$

Utilizing Green's Second Theorem gives

$$D_{eff} A \frac{\partial C}{\partial z} = \frac{U_0 D_M S E}{i \omega (S+1)} \frac{\gamma}{4} \cdot$$

$$\oint \left(\overline{g} \nabla f - g \nabla \overline{f} - f \nabla \overline{g} + \overline{f} \nabla g + \frac{i K D_M}{\omega \nu U_0} (\nabla \overline{g} + \nabla g) + \frac{K}{\omega^2 E} (\nabla \overline{f} - \nabla f) \right) dS \quad . \tag{3.40}$$

And using the boundary condition $\left.\frac{\partial g}{\partial \eta}\right|_{\eta = 1} = 0$ at the tube wall

yields

$$D_{eff} A \frac{\partial C}{\partial z} = \frac{U_0 D_M S E}{i \omega (S+1)} \frac{\gamma}{4} \oint \left\{ \left(\overline{g} - \frac{K}{\omega^2 E} \right) \nabla f - \left(g - \frac{K}{\omega^2 E} \right) \nabla \overline{f} \right\} dS \quad . \tag{3.41}$$

If two new functions are defined as $G(\eta) = 1 - \frac{\omega^2 E}{K} g(\eta)$ and $F(\eta) = i \frac{\omega U_0}{K} f(\eta)$, (Watson 1983) the integral is reduced in complexity to

$$D_{eff} A \frac{\partial C}{\partial x} = \frac{D_M S K^2 \gamma}{4\ (S+1)\ \omega^4} \oint (G \nabla \overline{F} + \overline{G} \nabla F)\, dS \tag{3.42}$$

where $dS = \eta\, d\theta$. This equation is solved simply as

$$D_{eff} A \frac{\partial C}{\partial x} = \frac{D_M S K^2 \gamma \pi}{2\ (S+1)\ \omega^4} \left(G(1)\ \frac{\partial \overline{F}(1)}{\partial \eta} + \overline{G}(1)\ \frac{\partial F(1)}{\partial \eta} \right) \tag{3.43}$$

where $G(1) = \left(1 - \frac{\omega^2 E}{K} g(1)\right)$ and $\frac{\partial \overline{F}(1)}{\partial \eta} = -i \frac{\omega U_0}{K} \frac{\partial \overline{f}(1)}{\partial \eta}$. It is interesting to note that since this is the sum of a function and its conjugate, the result is the real portion only.

$$G(1) = \frac{1}{(S-1)} \left(\frac{-\sqrt{S}\, J_1(\sqrt{-i}\, \alpha)\, J_0(\sqrt{-i}\, S\, \alpha)}{J_0(\sqrt{-i}\, \alpha)\, J_1(\sqrt{-i}\, S\, \alpha)} + S \right) \tag{3.44}$$

and

$$\frac{\partial \overline{F}(1)}{\partial \eta} = - \frac{\sqrt{i}\, \alpha\, \overline{J}_1(\sqrt{-i}\, \alpha)}{\overline{J}_0(\sqrt{-i}\, \alpha)} \ . \tag{3.45}$$

Multiplying equation 3.44 and equation 3.45 produces

$$G(1)\,\frac{\partial \overline{F}(1)}{\partial \eta} = \frac{1}{(1-S)}\left(\frac{-\sqrt{S}\,J_1(\sqrt{-i}\,\alpha)\,J_0(\sqrt{-i}\,S\,\alpha)}{J_0(\sqrt{-i}\,\alpha)\,J_1(\sqrt{-i}\,S\,\alpha)} + S\right)\left(\frac{\sqrt{i}\,\alpha\,\overline{J}_1(\sqrt{-i}\,\alpha)}{\overline{J}_0(\sqrt{-i}\,\alpha)}\right) . \tag{3.46}$$

Taking twice the real portion of equation (3.46) will provide the sum of the function and its conjugate of equation (3.43), namely

$$D_{eff} = \frac{K^2}{\alpha\,\omega^3\,(1-S^2)} \cdot \Re\left\{\left(\frac{-\sqrt{S}\,J_1(\sqrt{-i}\,\alpha)\,J_0(\sqrt{-i}\,S\,\alpha)}{J_0(\sqrt{-i}\,\alpha)\,J_1(\sqrt{-i}\,S\,\alpha)} + S\right)\left(\frac{\sqrt{i}\,\overline{J}_1(\sqrt{-i}\,\alpha)}{\overline{J}_0(\sqrt{-i}\,\alpha)}\right)\right\} . \tag{3.47}$$

Tidal Displacement Solution

The average tidal displacement can be calculated by taking the magnitude of the integral of one-half of the period times the area of the pipe and equating it to the tidal displacement times the area of the pipe. We have

$$\int_0^{2\pi}\int_0^1 \Delta x\,\eta\,d\eta\,d\theta = \left|\int_0^{\frac{\pi}{\omega}}\int_0^{2\pi}\int_0^1 U_0\,f(\eta)\,e^{i\omega t}\,\eta\,d\eta\,d\theta\,dt\right| , \tag{3.48}$$

$$\Delta x = \frac{4U_0}{\omega}\left|\int_0^1 \eta\,f(\eta)\,d\eta\right| , \tag{3.49}$$

and

$$\Delta x = \frac{4\,K}{\omega^2}\left|\int_0^1 \eta\left(1-\frac{J_0(\sqrt{-i}\,\alpha\eta)}{J_0(\sqrt{-i}\,\alpha)}\right)d\eta\right| . \tag{3.50}$$

Due to the fact that $\int x^n J_{n-1}(x)\,dx = x^n J_n(x)$ (Abramowitz and Stegan), upon integrating we find (Kurzweg 1988)

$$\Delta x = \frac{2K}{\omega^2}\left|1-\frac{2}{\sqrt{-i}\,\alpha}\left(\frac{J_1(\sqrt{-i}\,\alpha)}{J_0(\sqrt{-i}\,\alpha)}\right)\right| \tag{3.51}$$

or

$$K = \frac{\Delta x\ \omega^2}{2\left|1 - \dfrac{2\,J_1(\sqrt{-i}\,\alpha)}{\sqrt{-i}\,\alpha\,J_0(\sqrt{-i}\,\alpha)}\right|}\ . \qquad (3.52)$$

A plot of equation (3.52) relating axial pressure gradient K to tidal displacement is shown in Figure 3.10 and 3.11. Figure 3.12 is a phase relationship between the pressure gradient and velocity represented by

$$\Phi = Arg\left(1 - \frac{2\,J_1(\sqrt{-i}\,\alpha}{\sqrt{-i}\,\alpha\,J_0(\sqrt{-i}\,\alpha)}\right) \qquad (3.53)$$

Figure 3.10 Pressure-Displacement Relationship (Smaller α)

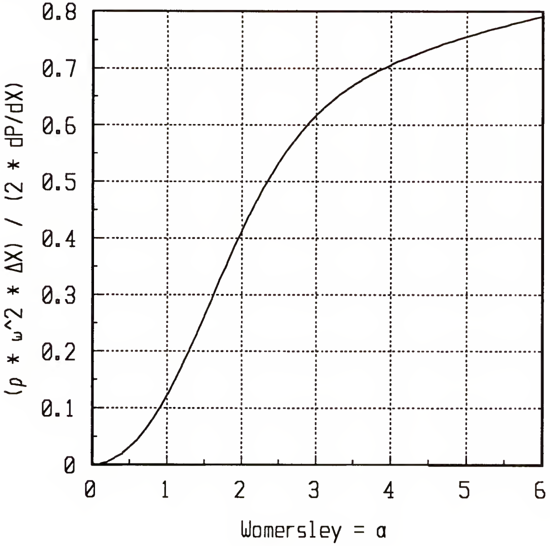

Figure 3.11 Pressure-Displacement Relationship (Larger α)

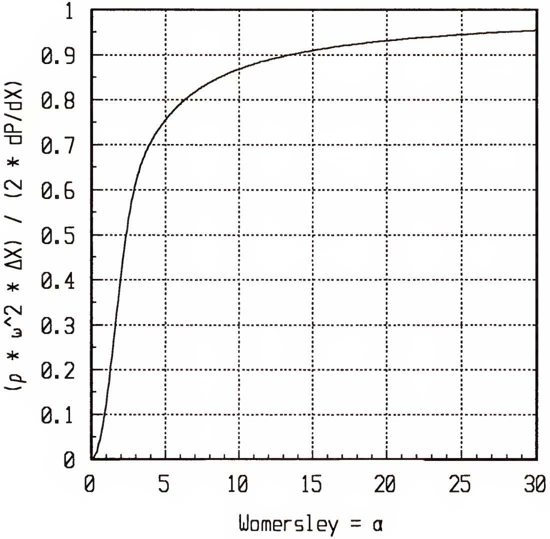

Figure 3.12 Phase between Pressure Gradient and Velocity

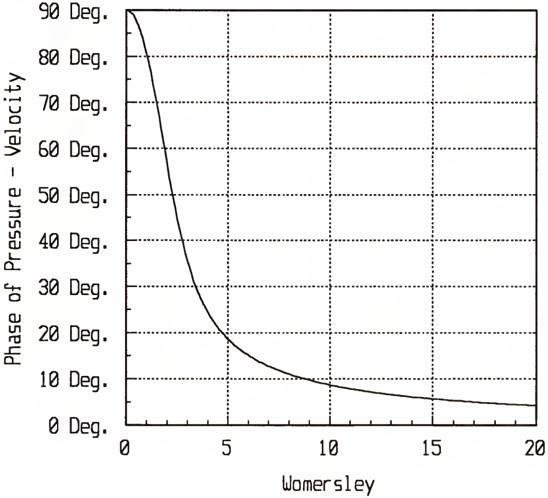

Enhanced Dispersion Coefficient in Final Form

Defining the non-dimensional dispersion coefficient $\lambda = D_{eff}/\omega \Delta x^2$, we have

$$\lambda(\alpha, S) = \frac{\Re\left\{\left(\frac{-\sqrt{S}\, J_1(\sqrt{-i}\,\alpha)\, J_0(\sqrt{-i\,S}\,\alpha)}{J_0(\sqrt{-i}\,\alpha)\, J_1(\sqrt{-i\,S}\,\alpha)} + S\right)\left(\frac{\sqrt{i}\,\bar{J}_1(\sqrt{-i}\,\alpha)}{\bar{J}_0(\sqrt{-i}\,\alpha)}\right)\right\}}{4\,\alpha\,(1 - S^2)\left|1 - \frac{2\,J_1(\sqrt{-i}\,\alpha)}{\sqrt{-i}\,\alpha\, J_0(\sqrt{-i}\,\alpha)}\right|^2} \qquad (3.54)$$

Now, letting

$$F(\alpha) = F_R(\alpha) + i\,F_I(\alpha) = i\,\frac{Ber_0'(\alpha) + i\,Bei_0'(\alpha)}{Ber_0(\alpha) + i\,Bei_0(\alpha)} = i\,\frac{J_0'(\sqrt{-i}\,\alpha)}{J_0(\sqrt{-i}\,\alpha)} = -i\,\frac{\sqrt{-i}\,J_1(\sqrt{-i}\,\alpha)}{J_0(\sqrt{-i}\,\alpha)}$$

equation (3.54) may be re-written in it's final desired form

$$D_{eff} = \frac{\Delta x^2\ \omega\ S}{4\,\alpha\,(S^2 - 1)}\left(\frac{F_I(\alpha) - \frac{|F(\alpha)|^2 F_I(\sqrt{S}\,\alpha)}{\sqrt{S}\,|F(\sqrt{S}\,\alpha)|^2}}{\left|1 + \frac{2\,F(\alpha)}{\alpha}\right|^2}\right) . \qquad (3.55)$$

This version for effective or enhanced dispersion coefficient in oscillatory flow was first obtained by Kurzweg and Jaeger (1987).

Graphical Presentation

Figure 3.13 is a contour plots of $\lambda = D_{eff}/\omega\Delta x$ as a function of Womersley Number α and Schmidt Number S. Two curves $\frac{\partial\lambda}{\partial\alpha} = 0$ and $\frac{\partial\lambda}{\partial S} = 0$ are plotted as well. $\frac{\partial\lambda}{\partial\alpha} = 0$ specifies the maximum value of λ for a given Schmidt number. $\frac{\partial\lambda}{\partial S} = 0$ specifies the maximum λ for a given Womersley Number. These curves are useful for studies involving the separation of species, showing, for example, that no diffusional separation will be possible when $\frac{\partial\lambda}{\partial S} = 0$.

Figure 3.13 Contour Plot of $\lambda = D_{eff}/\omega\ \Delta x^2$

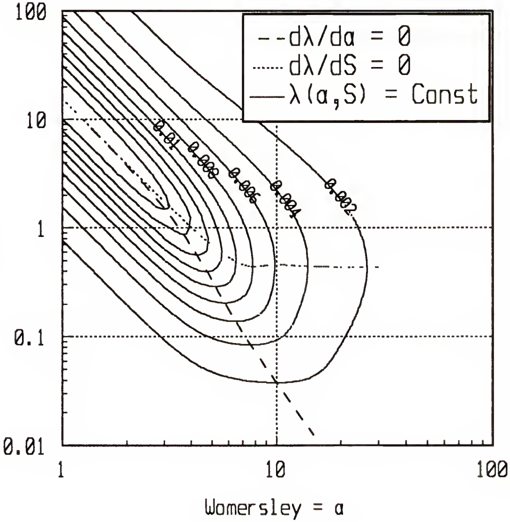

CHAPTER 4

EXPERIMENTAL PROCEDURE

In the previous Chapter we have derived the theoretical enhanced dispersion coefficient in oscillatory flow. This result will now be tested experimentally.

Enhanced Diffusion Process

Enhanced diffusion is a process by which a species in a fluid oscillating in a tube can experience a vastly amplified rate of axial dispersion as compared to that provided by normal molecular diffusion. This enhancement is promoted by an interaction between the boundary layer and the core as the fluid oscillates. The species under consideration is transferred first by diffusing radially into the boundary layer and later in the cycle diffusing, again radially, back into the oscillating core of the fluid, being transported axially a large distance from the originating location.

The enhancement is caused through an effective increase in diffusing surface area through the stretching action due to shear in the fluid, the boundary layer thickness, time allowed for diffusion to occur each cycle, and to a very limited degree an increase in the concentration gradient. This increase in concentration gradient can be visualized by considering, hypothetically, a tube with a linear concentration variation of one-hundred percent per one-hundred centimeter in a tube of two centimeter diameter. If the tidal displacement caused the core, which will remain at zero percent, to approach the area where the fluid at the tube wall will remain at one-hundred percent due to the no-slip requirement, the overall radial concentration gradient will now be one-hundred percent per centimeter.

The flow in an oscillating fluid is influenced by the pressure gradient, inertial forces, and viscous forces. The boundary layer thickness is determined by the frequency of oscillation and the kinematic viscosity of the fluid. As the frequency is increased, the boundary layer thickness is decreased. Likewise, the boundary layer thickness is decreased as the kinematic viscosity is decreased. This thickness influences the total amount of a species that it can contain. As the thickness of the boundary layer decreases, the capacity to hold a species is reduced due to the reduced mass of the boundary layer. The amount that the boundary layer will contain is also limited by the amount that a species that can diffuse into the boundary layer. There is a diffusion layer thickness that will contain the species that has diffused into the layer. If the boundary layer thickness is much greater than the diffusion thickness, little mass of the species will be contained in the boundary layer. Likewise, if the boundary layer is much less than the diffusion thickness, little mass will be transferred, due to the restriction of the boundary layer thickness. Therefore, there is a maximum mass transfer when the boundary layer thickness approximately matches the diffusion thickness. The amount of mass of a species transferred to the boundary layer is also influenced through the time allocated for transfer during a cycle. When the oscillating frequency is small, a larger time is allowed for a species to transfer to the boundary layer. This is one factor which determines the diffusion thickness. As the frequency is increased, the boundary layer thickness decreases, as well as the diffusion thickness decreasing due to the reduced time allowed for diffusion. The above peaking of the lambda curve (figure 3.13) is thus determined by the matching of boundary layer thickness to the diffusion thickness and leads to tuning effect first discussed by Kurzweg in 1986.

The pressure-velocity phase relationship (figure 3.12) is due to the relative change in importance of inertia and viscous forces. The ratio of inertial to viscous forces in oscillating pipe flow goes as the square of the Womersley number. The viscous forces are greater than inertial forces when the frequency is low. As the frequency is increased, the inertial forces increase faster than viscous forces, eventually overtaking them. These two forces are inherently 90° out of phase, therefore, the phase change is simply a result of the changing importance of the two forces.

The Pressure-Displacement curve (figure 3.10 and 3.12) is also a result of the phase change between the viscous forces and inertial forces. This curve is experimentally determined by measuring the magnitude of the pressure gradient, and the tidal displacement Δx of the fluid. Along with the fluid density, frequency of oscillation and tube radius, a curve can be generated. This curve is independent of the resonance of the system, therefore, it can be used to accurately infer the tidal displacement.

Experimental Procedure

The experimental procedure was to measure the enhanced diffusional flux, and calculate the associated enhanced axial dispersion coefficient. The diffusional flux was measured in two separate setups with frequency, tube radius, and tidal displacement varied over a wide range of values. The imposed constraints were to limit the tidal displacement to a maximum of one-third of the length of the tubes, and conditions set to remain in the laminar flow regime. To remain in the laminar regime a non-dimensional term $\Delta x \sqrt{\frac{\omega}{\nu}} < 800$ had to be met at all times. The turbulent range was determined by Kurzweg, Lindgren and Lothrop in 1989.

The diffusion flux rate was determined by measuring the concentration in the reservoirs with the associated flow rates. The measured diffusion coefficient can be obtained from the diffusional flux rate, cross-sectional area, length of tube, and the tidal displacement either measured directly, or from the measured magnitude of pressure gradient.

The experiment was performed on two different experimental setups shown in figures 4.1 through 4.3. The first used nitrogen from the atmosphere diffusing into oxygen. This apparatus was used to acquire initial operating experience with the equipment and for preliminary trial runs. The second, more sophisticated apparatus used by Dr. Jaeger for gas separation studies, was used here to obtain data on oxygen diffusing into carbon dioxide.

The first setup used a measure of pressure gradient instead of tidal displacement. This apparatus consisted of three different sized PVC tubes with two taps. These taps were located near the center of the tube in an attempt to reduce the influence of 'end effects' that consists of three major components. These are entrance turbulence, non fully formed velocity profiles and possible concentration gradient perturbations. The expected side effects of center taps along the length are reduced pressure differences and concentration differentials.

Figure 4.1 Schematic of Setup 1

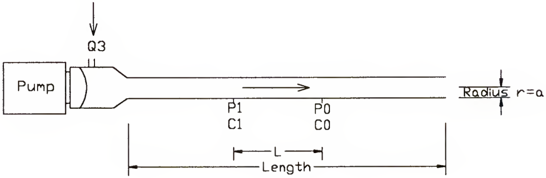

The second experimental apparatus consisted of a system of 76 glass capillaries, each being 0.38 centimeters in diameter and 120 cm in length. The tidal displacement was measured by means of a spirograph which had an electrical output proportional to the volumetric displacement. The measurement of tidal displacement was made independent of

Figure 4.2 Schematic of Setup 2

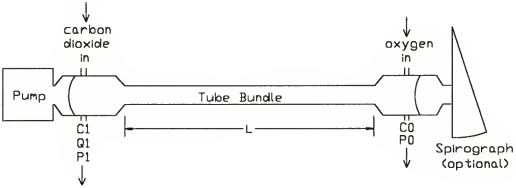

the actual diffusion test runs, as it was felt that the additional load on the system would affect the sinusoidal wave form and cause possible compressibility effects. It

Figure 4.3 Photograph of setup 2

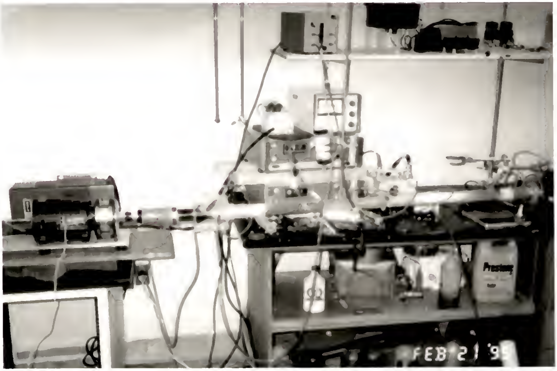

was not possible to obtain a true pressure gradient with the second setup due to the tube bundle construction, however, pressure was measured in the reservoirs and end effects were assumed to be minimal. Since the system had to be run as a closed system with oxygen diffusing into carbon dioxide, a more complex experimental apparatus was involved. Measurements of the inflow and outflow for each end reservoirs had to be measured and controlled.

EXPERIMENTAL ASSUMPTIONS

Diffusion Coefficient is Independent of Concentration

The Diffusion Coefficient does not change appreciably with concentration changes, but a minor change does occur (Bird 1960) (Hirschfelder, et al. 1949). Since this is a minor change, an assumption of constant molecular diffusion coefficient will not have a great influence in the final results.

Incompressible gases

The assumption that one is dealing with an incompressible gas was an assumption that was not quite met in this experiment, but closely approximated. The worst departure from the incompressible gas assumption occurs for the high tidal displacement and high frequency operation, as these are the conditions of greatest pressure gradient requirements. The great majority of the experimental runs had a pressure that fluctuated at most by 0.04 atmospheres.

Such conditions can be assumed to meet the incompressible gas condition.

The effects of compressibility include velocity changes due to the compression of the gas, the change in the molecular diffusion coefficient due to pressure changes, which will affect the Schmidt number.

Linear Concentration Gradient

Although the concentration gradient will vary in tubes where a counterflow exists, the concentration gradient can be considered as linear for a short length from any given plane normal to the tube axis. The actual concentration gradient in the first setup is an exponential curve along the length of the tube. In the second setup, the concentration gradient is in fact linear. This assumption is best approximated when the tidal displacement is small.

Pressure Gradient is a Function of a Pure Sine Wave in Time

A large problem in this experiment was in generating pure sine waves. A linear motor was used to generate a pure driving sine wave, shown in figure 4.4, but there were two separate causes of harmonics in this experiment. One is the acoustic frequency of the tube and the other is the tube and isolator coupling.

Figure 4.4 Photograph of Linear Motor Used to Produce Sinusoidal Axial Displacements of Fluid within Conduit.

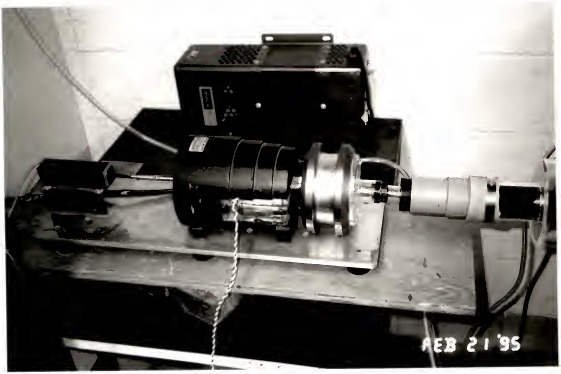

The acoustic frequency of the tube is caused by a one-quarter wavelength, or an odd multiple of a quarter wavelength, pressure wave standing in the tube. This is controlled largely by the physical length of the tube. Lengthening of the tube causes a lowering of the acoustic frequency. Mathematically, the acoustic frequency , i.e.

Figure 4.5 Photograph of Pressure Variation (Top)
and Tidal Volume (Bottom)

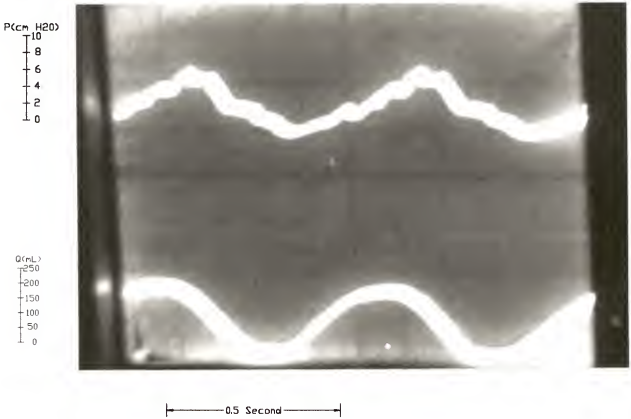

the quarter wave, is $\omega = \frac{c}{4L}$, where c is the acoustic velocity and L is the length of the tube.

Another cause of harmonics is from a coupling of the tube and the end chambers. This frequency is caused from the compressibility of the gas in the end chamber acting on the mass of the gas oscillating in the tube. In the non-viscous case, this frequency is directly proportional to the diameter of the tube and inversely proportional to the square root of both the length of the tube and the volume of the isolation chamber. The non-viscous natural frequency is $\omega = \frac{ac\sqrt{\pi}}{\sqrt{LV}}$ where a is the radius of the tube, c is the speed of sound, L is the length of the tube and V is the volume of the isolation chamber.

The acoustic frequency provided high frequency harmonics generally of the tenth order that caused the driving frequency to have imposed upon it this tenth order harmonic. (See Figure 4.5) The tube-isolation chamber frequency was of the same order of frequency as the driving frequency, the main problem being a resonance that causes the tidal displacement to be much larger than it otherwise would have been. Since the pressure gradient is related to the tidal displacement, no adverse effect was observed by this when using the pressure-tidal displacement measurement, provided the waveform remained as a pure sine wave.

The acoustic frequency was the larger of the two problems when the driving frequency was high. The solution was to use a short length of tube, forcing the acoustic frequency to become very high. The effects eventually became negligible when a short tube was used. At low frequencies, the isolator-tube coupling was the larger problem. There was no solution to this problem for the equipment on hand except to keep the operating frequency above the point where the harmonics became dominant.

Cross-Sectional Velocity Profile is Fully Developed

Taking pressure gradient measurements near the center of the tube length insures that the velocity profile is as fully developed as can be obtained in this experiment. This is one of the 'end effects' problems mentioned earlier. Indications from earlier studies (Kurzweg, Lindgren and Lathrop 1989) indicate end effects in tube length only extend about Δx distance along the tube from their ends.

Transverse Diffusion Effects Overwhelms Axial Diffusion

Transverse diffusion is assumed in the theoretical development to be the only component of molecular diffusion involved in producing of the enhanced diffusion. Since the enhanced diffusion is several orders of magnitude larger than molecular diffusion, this is generally a safe assumption. This will not be true in exceptionally low Womersley Number or extremely high Womersley Number conditions, where the lambda is very low as is suggested by

Figure 3.13. In these cases, the enhanced diffusion may be comparable to molecular diffusion.

Flow is Completely Laminar

It is assumed that the flow is completely laminar everywhere. The effects of turbulence are not completely understood in enhanced dispersion. Since self-maintaining turbulence in oscillating flow generally develops slowly, the effects of some limited end effect turbulence are possibly negligible, but must not be forgotten (Kurzweg, Lindgren and Lothrop 1989).

Steady State Conditions have been Achieved

The measurements made in this experiment are only valid for steady state laminar conditions. The various measurements were observed to ensure that steady state conditions were attained. Small deviations from steady state conditions possibly will not affect the outcome appreciably. This may not be the case if obvious non-steady state conditions exist. In the first setup, steady state conditions sometimes took as long as six hours to attain, and therefore, a few readings may have been made before steady state conditions had actually occurred.

Tube is Completely Straight

The tube is kept as straight as possible to reduce the effects of accelerations cause by the deviations. These accelerations will affect the flow characteristics of the fluid that will invalidate the theory developed for this experiment. Previous investigators have found that tube curvature increases the rate of diffusion (Sharp et al. 1991).

All Measurements are Accurate

The calibration of the various pieces of equipment used in this experiment were calibrated as follows. The flow rate of the feed gas was measured with a flow meter that was calibrated by measuring the volume delivered over a specified time. The flow was calibrated at steady atmospheric conditions. The frequency was checked at low frequency and assumed to remain consistent as the frequency was increased. The tube radius was measured using a caliper and averaging the measurement over various angular measurements. A water column was used to calibrate the pressure transducer. Although this is a static measurement, it is assumed that the calibration will remain valid for transient measurements. The concentration measurement could be easily calibrated at zero and atmospheric conditions only in the first setup, at zero and one hundred percent for the second setup. The meters were assumed to be linear in their output, as no easy way to calibrate for intermediate concentrations was found.

No Leaks To or From Tube System

One large problem early in the experiments, was a diaphragm used in the isolation end chamber. This diaphragm was necessary to prevent atmospheric gases from leaking in or experimental gases from leaking out of the reservoir area of the isolator through the pump piston. Originally, Reynold's Wrap was used as the diaphragm material, but was found to allow the gases to diffuse directly through this diaphragm material, invalidating the data collected. The next diaphragm used was some thin rubber material. It was found to be too flexible, allowing the inlet to become sealed with the diaphragm material during part of the cycle. A composite diaphragm was used for the remainder of the experiment. This diaphragm was constructed of three layers, the two outer layers were Reynold's Wrap with the inner layer being thin rubber material. This composite diaphragm met the requirements of being impenetrable to gas diffusion through the material plus had an appropriate strength.

Tidal Displacement Remains Small

The tidal displacement must remain small compared to the length of the tube to insure that flushing of the tube is kept at a minimum. If the tidal displacement were to get excessively large exceeding the length of the tube, there would be, in addition to enhanced diffusion, considerable axial convection. To insure that some unflushed gases remain in the tube, a limit of one-third the tube length for tidal displacement was arbitrarily chosen as the upper limit used.

Deriving the Non-dimensional Expressions Used in the Experimental Measurements of the Two Setups

The first setup had a net flow into the tube which balanced the upstream diffusion. This flow was caused by the injection of pure oxygen into the reservoir. This causes the axial concentration to deviate from the usual linear concentration variation. A method has to be developed to get a numerical value for the enhanced diffusion coefficient.

The diffusion in the first experiment is balanced by an equal and opposite convective flow. Thus at mean velocity

U_0 one has

$$U_0\, C = D_{eff} \frac{\partial C}{\partial z} \quad . \tag{4.1}$$

The general solution to this equation is

$$C = A\, e^{\frac{U_0\, z}{D_{eff}}} \quad . \tag{4.2}$$

To solve for the Effective Diffusion D_{eff}, the log of the above equation is taken. One has

$$\ln(C) = \ln(A) + \frac{U_0\, z}{D_{eff}} \quad . \tag{4.3}$$

Boundary conditions of $C(0) = C_0$ and $C(L) = C_1$ are applied resulting in

$$D_{eff} = \frac{U_0\, L}{\ln\left(\frac{C_1}{C_0}\right)} \quad . \tag{4.4}$$

The velocity is determined by the volumetric flow rate of gas into the isolation chamber

$$D_{eff} = \frac{\dot{Q}\, L}{A \ln\left(\frac{C_1}{C_0}\right)} \tag{4.5}$$

where $\dot{Q}$ is the volumetric flow rate of the gas into the isolation chamber, L is the length between sample ports, A is the cross-sectional area of the tube and C_0, C_1 are the concentration measurements at the two sample ports. (See Figure 4.1)

The Effective Diffusion Coefficient equation derived in Chapter 3 is difficult to use with the first experimental setup due to the fact that we are measuring the pressure gradient instead of measuring the tidal displacement. Since the measured quantity is the pressure gradient, it is easier to recast the equation into components using the pressure gradient measurement. Taking the original function for D_{eff} given by equation 3.47, namely

$$D_{eff} = \frac{\left|\frac{1}{\rho}\frac{\partial P}{\partial x}\right|^2}{\alpha\,\omega^3\,(1 - S^2)} \cdot \Re\left\{\left(\frac{-\sqrt{S}\,J_1(\sqrt{-i}\,\alpha)\,J_0(\sqrt{-i}\,S\,\alpha)}{J_0(\sqrt{-i}\,\alpha)\,J_1(\sqrt{-i}\,S\,\alpha)} + S\right)\left(\frac{\sqrt{i}\,\bar{J}_1(\sqrt{-i}\,\alpha)}{\bar{J}_0(\sqrt{-i}\,\alpha)}\right)\right\}, \qquad (4.6)$$

a new function N can be defined as

$$N(\alpha, S) = \frac{\Re\left\{\left(\frac{-\sqrt{S}\, J_1(\sqrt{-i}\,\alpha)\, J_0(\sqrt{-i\,S}\,\alpha)}{J_0(\sqrt{-i}\,\alpha)\, J_1(\sqrt{-i\,S}\,\alpha)} + S\right)\left(\frac{\sqrt{i}\,\bar{J}_1(\sqrt{-i}\,\alpha)}{\bar{J}_0(\sqrt{-i}\,\alpha)}\right)\right\}}{4\,\alpha\,(1 - S^2)} , \tag{4.7}$$

resulting in

$$N(\alpha, S) = \frac{\rho^2\,\omega^3\,D_{eff}}{4\left|\frac{\partial P}{\partial x}\right|^2} . \tag{4.8}$$

Substituting equation (4.5) for D_{eff} and recasting in experimentally derived terms, yields

$$N(\alpha, S) = \frac{\dot{Q}\,L\,\rho^2\,\omega^3}{4\,A\,\ln\left(\frac{C_1}{C_0}\right)\left|\frac{\partial P}{\partial x}\right|^2} . \tag{4.9}$$

Some reasonable approximations can be made to convert this into measurable quantities. The pressure gradient can be approximated as $\frac{\partial P}{\partial z} = \frac{P_1 - P_0}{L}$ where L is the interval between pressure ports in setup one and $A = \pi\,a^2$ is the tube cross-sectional area. Thus we arrive at the desired non-dimensional expression

$$N(\alpha, S) = \frac{Q L^3 \rho^2 \omega^3}{4 \pi a^2 (P_1 - P_0)^2 \ln\left(\frac{C_1}{C_0}\right)} \tag{4.10}$$

A plot of N(α,S) is shown in Figure 4.6. It again shows

Figure 4.6 Contour Plot N(α,S)

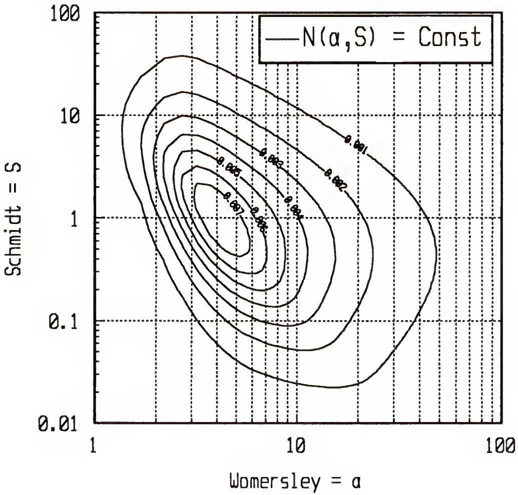

a tuning effect with maximum values of N occurring near $S = 1$ and $\alpha = 4$.

In the second experimental setup, no net flow was the desired condition, therefore, the diffusion equation is simply

$$\frac{\partial^2 c}{\partial x^2} = 0 \qquad (4.11)$$

or

$$\frac{\partial c}{\partial x} = Constant \quad . \qquad (4.12)$$

The enhanced diffusion coefficient is therefore simply

$$D_{eff} = \frac{\dot{Q}_1 \, C_1 \, L}{(C_0 - C_1) \, A} \quad , \qquad (4.13)$$

where Q_1 is the low concentration outflow, C_0 and C_1 are the high and low concentration respectively at the capillary ends, L is the length of the tubes and A is the total tube cross sectional area.

The enhanced dispersion equation (3.55) is equated to this to obtain an experimentally determined value for lambda of

$$\lambda(\alpha, \sigma) = \frac{\dot{Q}_1 C_1 L}{A \, (C_0 - C_1) \, \Delta x^2 \, \omega} \quad . \qquad (4.14)$$

Determining Density and Viscosity Experimentally

It is interesting to note that by performing the pressure-displacement experiment, both the density and viscosity coefficient of a gas under study can be determined. The process best fits the collected data to the pressure-displacement curve with a least sum-of-squares on both parameters density and viscosity, which will provide the density and kinematic viscosity directly.

Another method utilizes the inflection point of the pressure-displacement curve. The inflection point of this curve is at a Womersley Number of 1.62 with the corresponding function value of 0.298. This method would best fit the data to a quartic function that will provide an inflection point. If sufficient data can be collected, the inflection point can be determined, assuming that the pressure gradient, frequency, tidal displacement, and tube diameter are known. This inflection point will provide the information to deduce the density and kinematic viscosity.

Both of the above methods assume that the gas under test does not have any change of properties along the tube length during the test, which is difficult to attain experimentally.

With the non-dimensional parameters and theoretical functions derived, the experimental data can be evaluated. The results of the experiment are presented in the next chapter.

CHAPTER 5

EXPERIMENTAL RESULTS

Setup One

The first experimental setup was run using oxygen as the carrier gas and nitrogen in air as the upstream diffusing gas. These gases were chosen as best for this experiment because the densities and kinematic viscosities did not vary between the gases appreciably and were gases readily available. The raw data will be presented as well as the computed results. Two isolators (end chambers) were available during these experiments. These isolators separated the pump from the tube, insuring that no gas leaked into or out of the pump. The data was collected using the larger of the two isolators, due to the isolator-tube induced harmonics at low frequencies for the smaller isolator.

Achieving steady state conditions in some of the test runs, sometimes required over six hours. Because of this long time span, it was difficult to determine if a steady state condition in fact was achieved. Some deviations in the results are possible because of non-steady state conditions being accepted as steady state. At times, large concentration surges that were short lived were observed during recording. It was not possible to determine if this was due to turbulence, a concentration wave passing through the tube, poor mixing in the reservoirs, or any other reason. The test runs that had exhibited obvious large concentration surges were discarded.

Repeating these experiments using other carrier gases was not possible due to the large sampling requirements of the available oxygen and helium concentration meters. Even the small sampling requirements of the nitrogen concentration meter affected the results of this experiment. The sampling meter could not be connected to the ports continuously, as this affected the concentration in the tube. Instead, the sampling probe had to be inserted temporarily to obtain a reading and removed to retain the concentration in the tube.

Highly repeatable concentration readings were not possible for an unknown reason, therefore, an averaged reading was used to reduce the effects of the variance of the readings. It was felt that an average of the actual concentration readings was superior to averaging the ratio of the individual reading since the concentration readings were not instantaneous readings, but reading taken a short time interval apart.

The pressure transducer was calibrated using a water column, obtaining 27.6 cm of water for 30 divisions on an oscilloscope on a scale of 0.5 volts per division. This results in a pressure of 1.84 cm of water per volt as the calibration of the pressure transducer. The pressure measured was peak-to-peak pressure, therefore, half of this value was used as the amplitude of the pressure in the pressure gradient measurement.

The three tubes used were each 153 cm in length. The tubes had radius measurements of 0.587 cm, 0.777 cm and 1.03 cm. The kinematic viscosity used for calculations was ν = 0.16 cm squared per second. The pressure ports were 30.5 cm apart, 61 cm from each end and flush to slightly recessed from the inner surface of the tube.

Table 5.1 Raw Data - Setup 1

Test Number	Radius cm	Freq Hz	$P_1 - P_0$ div	Scale V/div	C_0 %	C_1 %	$\dot{Q}$ L/Min
1	0.587	3.5	30.6	0.02	59.0 62.4 59.4 58.0 57.5 62.7	43.0 42.0 41.9 43.8 40.8 43.9	0.25
2	0.587	5.0	18.8	0.05	51.5 50.5 53.0 49.0 55.0	35.6 38.5 33.2 37.9 34.5	0.25
3	0.587	6.0	15.0	0.05	41.1 46.0 43.8 45.6 45.5	30.6 31.3 31.6 31.1 31.6	0.10
4	1.03	7.0	22.5	0.05	52.0 53.1 48.5 45.7 48.8	36.1 38.2 32.0 32.5 31.1	0.25
5	1.03	10.0	22.5	0.05	41.8 39.4 35.8 42.6 35.4	23.0 23.2 21.4 23.1 17.5	0.50
6	0.777	5.0	10.8	0.10	73.2 72.0 73.0 72.0 73.4	64.2 62.4 60.1 59.5 63.0	0.25
7	0.777	6.0	24.0	0.05	44.2 41.7 43.7 41.0 43.9	28.1 25.0 28.8 21.4 27.2	0.50
8	0.777	5.0	10.0	0.05	19.8 19.0 19.2 19.4 19.5	9.8 10.1 10.2 9.9 9.5	0.10
9	0.777	10.0	17.0	0.10	47.0 41.0 46.5 44.9 45.6	34.2 30.2 34.8 35.8 35.1	0.10

The results shown in Table 5.2 show a relatively large error, low for smaller Womersley numbers and high for larger Womersley numbers. The lower values are possibly in error due to steady state conditions not occurring. The nearly consistent error for the higher values is of unknown origin. Because the experimental N values are above all possible N function values for these Womersley Numbers, a minimum error by least sum-of-squares is meaningless. This experimental test run sequence was thus of no value in determining an experimental value of diffusion coefficient. The test setup was unable to get any lower than a Womersley Number of 6.8, due to pressure gradient measurements limitations.

Table 5.2 Results Setup 1

Test Number	Womersley Number	N_{exp}	N_{theory}	N_{exp} % Error	$\frac{D_{eff_{exp}}}{D_M}$	ΔX_{calc} cm
4	6.88	0.00402	0.00595	-32.4	1617	50.86
2	8.22	0.00463	0.00511	-9.4	1508	39.58
4	9.01	0.00523	0.00472	10.8	627	22.26
4	17.08	0.00277	0.00262	5.7	471	26.41
5	20.41	0.00260	0.00221	17.6	606	26.23
6	11.93	0.00415	0.00367	13.1	1940	45.64
7	11.93	0.00412	0.00367	12.3	1265	37.00
8	13.77	0.00370	0.00321	15.3	187	13.22
9	15.40	0.00338	0.00289	17.0	450	19.38

We note, however, that quite large values of D_{eff}/D_M where found. Such large increases support the theoretical predicted values.

Figure 5.1 Experimental Data Setup 1

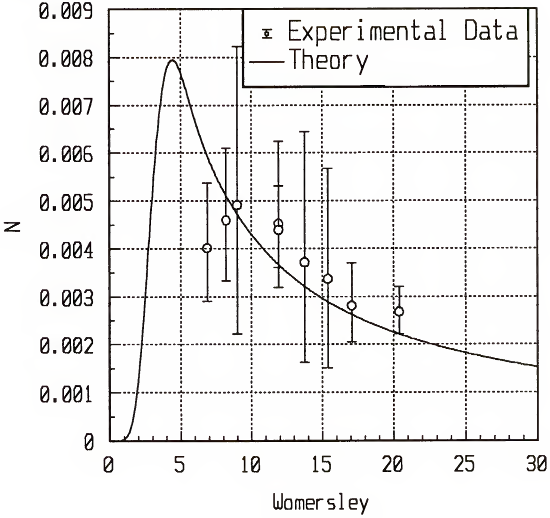

Setup Two

In the second setup, a capillary system of 76 glass tubes in a close-packed bundle each 0.38 cm in diameter were used. These tubes emptied into reservoirs on each end which had inlet and outlet connections. The tidal displacement was measured using a spirograph which was connected separately from the actual test to reduce the compressibility effects from the additional load on the test. The flow rate of each connection had to be measured, attempting to minimize the net flow in the tubes themselves. All of these measurements were conducted in static conditions. The settling time for this experimental setup was much quicker than the first setup, being on the order of five minutes. This was due to the smaller diameter tubes, the larger total tube area, smaller reservoirs, and larger feed rates of the gases. Table 5.3 presents the raw data that was collected during the operation of the second setup.

Table 5.3 Raw Data Setup 2

Test Run	Freq Hz	$\dot{Q}_3$ ml/s	C_0 %	C_1 %	ΔX cm
14	5	500	50.6	35.3	25.1
14	5	520	51.4	35.3	25.1
12	10	520	46.6	41.4	33.0
14	1	520	74.0	5.0	22.7
14	1	520	72.5	4.9	22.7
15	10	530	47.6	41.8	33.0
16	2.5	500	55.9	20.0	23.2

Table 5.4 presents the calculated results with the error in each run. The values of Womersley number is based on the kinematic viscosity of the carrier fluid being entirely carbon dioxide (0.085 cm^2/s), and the theoretical lambda value based on the Schmidt number being the reference value of 0.518, taken from tables 2.1 and 2.2.

Table 5.4 Results Setup 2

Test Number	Womersley Number	λ_{exp}	λ_{theory}	λ_{exp} % Error	$\frac{D_{eff_{exp}}}{D_M}$
12	3.653	0.0[illegible]35	0.0127	6.3	1629
11	3.653	0.0133	0.0127	4.7	1605
12	5.166	0.0140	0.0127	9.4	5841
13	1.634	0.0027	0.0035	-22.9	53.3
14	1.634	0.0027	0.0035	-22.9	53.3
15	5.166	0.0129	0.0128	0.8	5382
16	2.583	0.0076	0.0081	-6.2	392

Figure 5.2 Results Setup 2

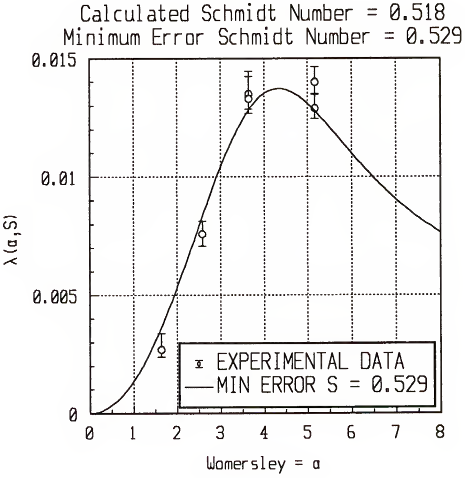

The large error in test runs 13 and 14 is most likely due to an error in concentration measurement at the low concentration reading. Because there is a relatively small diffusional flux in these test runs, an error in the concentration reading will be greatly amplified. Another likely reason is because of the great concentration change over the length of the tube. If the actual diffusion coefficient remains constant, the Schmidt number will change by a factor of nearly two over the length of the tube, due to the viscosity change of the gas mixture.

An estimate of the Schmidt number can be determined by a least sum-of-squares of error between the theoretical curve and collected data. The least error by this method was determined to be a Schmidt number of 0.529. This value implies a coefficient of diffusion of 0.161 cm^2/s. This compares very favorably to the tabulated value of 0.164 cm^2/s at the same conditions. When reduced to standard tabulated conditions of 0°C and one atmosphere, the determined value is 0.136 cm^2/s compared to the tabulated value of 0.139 cm^2/s.

The error bars shown in figures 5.1 and 5.2 were computed using one-half of the resolution on each measurement, calculating the worst case condition for high and low respectively.

Pressure-Displacement

The pressure-displacement equation 5.1, namely,

$$\frac{\rho\omega^2\Delta x}{2\left|\frac{\partial P}{\partial x}\right|} = \left|1 - \frac{2\sqrt{i}\,J_1(\sqrt{-i}\alpha)}{\alpha\,J_0(\sqrt{-i}\alpha)}\right| \tag{5.1}$$

was verified using air in the tube. The tidal displacement was measured using a spirograph. This was calibrated by injecting into the system a measured volume of gas and noting the output voltage from the spirograph. The pressure gradient was determined by measuring the pressure in the reservoir and dividing this by the length of the tube. Although this is not a true measurement of pressure gradient, the tube entry losses were estimated to be minimal, with the greatest pressure drop from the flow in the tube. The pressure transducer was calibrated with a water column. The density used was a tabulated value of 1.177 Kg/m^3. The volume is listed as divisions noted on the oscilloscope with a conversion factor of 15.7 cm/div. The pressure gradient is also listed in divisions peak-to-peak as noted on the oscilloscope with a conversion factor of 0.0000266 atm/(cm div). With the exception of the last entry, all data was collected in the second setup. The minimum Womersley number that was obtainable with reasonable results in setup one was about 6.8, due to the method of obtaining Δx. Δx was measured by a pressure increase in a large bottle.

Table 5.5 Pressure-Displacement Results

Hz	Δx div	Press. Grad. div	Womersley	$\frac{\rho\omega^2\Delta x}{2\left\lvert\frac{\partial P}{\partial x}\right\rvert}$	Theory
1	1.45	0.3	1.203	0.1308	0.1757
5	1.6	1.9	2.691	0.5698	0.5703
10	2.1	7.9	3.806	0.7195	0.6935
3.5	*	36	6.793	0.8050	0.8126

Figure 5.3 Experimental Data Pressure-Displacement Relationship

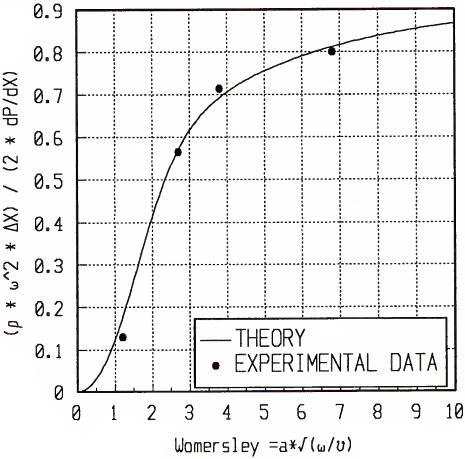

CHAPTER 6

CONCLUSIONS

Concluding Remarks

This experiment proved that the Molecular Diffusion Coefficient in gases can be determined by means of the enhanced dispersion in oscillatory flow. Ideally, data for a large range of Womersley numbers can be collected and this will provide a very precise determination of the Schmidt number from which the molecular diffusion coefficient then is found. This ensures that the one correct lambda, or N curve as a function of Schmidt number is selected and reduces the statistical standard deviation from a large sampling. Once this Schmidt number is found, the molecular diffusion coefficient can be determined by dividing the carrier fluid's kinematic viscosity by the Schmidt number. In the discussion here, lambda will be used, but the same conclusions also apply to the N function.

If only a small range, or small sampling of Womersley number can be obtained, from either equipment limitations or any other causes, the range of collected data will be most sensitive for Womersley number near the tuning point. That is, the most sensitive data occurs near $\frac{\partial \lambda}{\partial \alpha} = 0$, which corresponds to the peak of the lambda function. This is so critical because it will allow a check of the measured value of lambda itself which is not possible on other limited ranges of the lambda curve. If sufficient data is collected to specify the actual peak of this curve, the appropriate Schmidt number can be determined directly.

The second best limited range for gases is in the range of Womersley numbers below the peak, where $\frac{\partial\lambda}{\partial\alpha} > 0$. This selection is desirable because, as a function of Schmidt number, the lambda function near the desired Schmidt number is always monotomically increasing. This allows for far better discrimination of the Schmidt number using the least sum-of-squares of error procedure.

The least desirable location for data points is above the peak of the lambda curve, or $\frac{\partial\lambda}{\partial\alpha} < 0$. In this location, the function is not necessarily monotomic as a function of Schmidt Number.

The greatest problem in determining the diffusion coefficient with this method is in determining the tidal displacement. Because this term is squared in the experimental determination of lambda, any error is greatly amplified. In practice, the determination of N should be more precise than lambda, due to the generally more precise measurement of the magnitude of pressure gradient instead of tidal displacement.

Although this procedure appears to work well with gases, in liquids it may be far less desirable. Liquids generally have Schmidt numbers on the order of 1000, whereas in most gases it is near 0.7. With the Schmidt number this large, the lambda curve peaks well below a Womersley number of one. In this range, there is very little distinction between different lambda curves as a function of Schmidt number, therefore, a precise determination of Schmidt number becomes much more difficult.

It is interesting that the presented method for determining D_M is found to be quite accurate for gases and thus offers an alternative to the standard Loschmidt approach for determining this important constant experimentally.

Future Work

Future work should involve a study of the effect of harmonics on the observed enhanced dispersion considered here. The collected data with setup one, suspects that harmonics may increase the effective diffusion in the range of Womersley Number greater than the tuning point of the λ curve.

Some consideration should also be given to the use of transient changes in concentration at a specific location within the confining tubes. Such an approach would allow not only a more rapid determination of D_M but also would allow extension of the present method to high Schmidt number fluids such as liquids.

APPENDIX

```
CCCCCCCCCCCCCCCCCCCCCCCCCCCCCCCCCCCCCCCCCCCCCCCCCCCCCCCCCCCC
C                                                          C
C CALCULATES LAMBDA GIVEN THE WOMERSLEY AND SCHMIDT NUMBERSC
C                          AND                             C
C   CALCULATES N GIVEN THE WOMERSLEY AND SCHMIDT NUMBER    C
C                                                          C
C WOMERSLEY NUMBER = RADIUS OF TUBE TIMES SQUARE ROOT OF   C
C                    QUANTITY ANGULAR FREQUENCY OVER       C
C                    DYNAMIC VISCOSITY                     C
C                                                          C
C SCHMIDT NUMBER = DYNAMIC VISCOSITY OF CARRIER GAS        C
C                  OVER MOLECULAR DIFFUSION COEFFICIENT    C
C                  OF TRACE GAS INTO CARRIER GAS           C
C                                                          C
CCCCCCCCCCCCCCCCCCCCCCCCCCCCCCCCCCCCCCCCCCCCCCCCCCCCCCCCCCCC
      DOUBLE PRECISION FAC(0:80), A, S, LAM, N
      INTEGER I
      COMMON FAC
      WRITE(*,*)'Enter a value for Womersley Number (A)'
      READ(*,*) A
      WRITE(*,*)'Enter a value for Schmidt Number (S)'
      READ(*,*) S
      FAC(0) = 1D0
      DO 10 I = 1, 80
      FAC(I) = FAC(I-1) * I
10    CONTINUE
      IF (SQRT(S) * A .GT. 85D0 .OR. A .GT. 85D0) THEN
      WRITE(*,*)
      WRITE(*,*)'POSSIBLE ERROR DUE TO EXCEEDING THE MAXIMUM
     #ALLOWABLE FOR THIS APPROXIMATION'
      WRITE(*,*)'THE MAXIMUM FOR A, OR SQRT(S) * A IS 85'
      ENDIF
      WRITE(*,*)
      WRITE(*,*)'(Womersley)  (Schmidt)'
      WRITE(*,*)'     A           S            LAMBDA(A,S)
     #  N(A,S)'
      WRITE(*,101)A, S, LAM(A, S), N(A, S)
101   FORMAT(3X, F6.3, 5X, F6.3, 6X, F18.16, 2X, F18.16)
      END
```

```
CCCCCCCCCCCCCCCCCCCCCCCCCCCCCCCCCCCCCCCCCCCCCCCCCCCCCCCCCCCC
C                                                          C
C  SUBROUTINE TO CALCULATE LAMBDA AS A FUNCTION OF BESSEL  C
CFUNCTIONS WITH PARAMETERS OF WOMERSLEY AND SCHMIDT NUMBERSC
C                                                          C
CCCCCCCCCCCCCCCCCCCCCCCCCCCCCCCCCCCCCCCCCCCCCCCCCCCCCCCCCCCC
      DOUBLE PRECISION FUNCTION LAM(A, S)
      DOUBLE PRECISION A, S
      DOUBLE COMPLEX SRNI, J, J0, J1, J0S, J1S
      SRNI = CDSQRT( (0D0,-1D0) )
      J0 = J(0, SRNI * A)
      J1 = J(1, SRNI * A)
      J0S = J(0, SRNI * DSQRT(S) * A)
      J1S = J(1, SRNI * DSQRT(S) * A)
      LAM = DBLE(( -DSQRT(S) * J1 * J0S / (J0 * J1S) + S) *
     #CDSQRT( (0D0,1D0) ) * DCONJG(J1) / DCONJG(J0)) /
     #(4D0 * A * (1D0 - S ** 2) * (CDABS(1D0 - 2D0 * J1 /
     #(SRNI * A * J0)) ** 2))
      RETURN
      END
```

```
CCCCCCCCCCCCCCCCCCCCCCCCCCCCCCCCCCCCCCCCCCCCCCCCCCCCCCCCCCCC
C                                                          C
C    SUBROUTINE TO CALCULATE N AS A FUNCTION OF BESSEL     C
CFUNCTIONS WITH PARAMETERS OF WOMERSLEY AND SCHMIDT NUMBERSC
C                                                          C
CCCCCCCCCCCCCCCCCCCCCCCCCCCCCCCCCCCCCCCCCCCCCCCCCCCCCCCCCCCC

      DOUBLE PRECISION FUNCTION N(A, S)
      DOUBLE PRECISION A, S
      DOUBLE COMPLEX SRNI, J, J0, J1, J0S, J1S
      SRNI = CDSQRT( (0D0, -1D0) )
      J0 = J(0, SRNI * A)
      J1 = J(1, SRNI * A)
      J0S = J(0, SRNI * DSQRT(S) * A)
      J1S = J(1, SRNI * DSQRT(S) * A)
      N = DBLE( ( -DSQRT(S) * J1 * J0S / (J0 * J1S) + S) *
     #CDSQRT( (0D0,1D0) ) * DCONJG(J1) / DCONJG(J0)) /
     #(4D0 * A * (1D0 - S ** 2))
      RETURN
      END
```

```
CCCCCCCCCCCCCCCCCCCCCCCCCCCCCCCCCCCCCCCCCCCCCCCCCCCCCCCCCCCC
C                                                          C
C     SERIES REPRESENTATION OF THE BESSEL FUNCTION         C
C                                                          C
C     V = ORDER OF FUNCTION                                C
C     X = POINT TO BE EVALUATED                            C
C                                                          C
C     VALID FOR ABS(Y) < 85 WHEN X = Y * SQRT(-I)          C
C                                                          C
CCCCCCCCCCCCCCCCCCCCCCCCCCCCCCCCCCCCCCCCCCCCCCCCCCCCCCCCCCCC

      DOUBLE COMPLEX FUNCTION (V, X)
      DOUBLE COMPLEX X, J1
      DOUBLE PRECISION FAC(0:80)
      INTEGER V, I
      COMMON FAC
      J1 = (0D0,0D0)
      DO 10 I = 0,79
      J1 = J1 + ( -1D0) ** I * (X / 2D0) ** (2 * I + V) /
     #(FAC(I) * FAC(I + V))
10    CONTINUE
      J = J1
      RETURN
      END
```

REFERENCES

Abramowitz, M., and Stegan, I. A., HANDBOOK OF MATHEMATICAL FUNCTIONS 9th ed, Dover, New York (1972)

Aris, R. "On the dispersion of a solute flowing through a tube" Proc. Roy. Soc. A 235 67 (1956)

Bird, R. B., Stewart, W. E., Lightfoot, E. N. TRANSFER PHENOMENA John Wiley & Sons, New York, (1960)

Chapman, S., Cowling, T. G., THE MATHEMATICAL THEORY OF NON-UNIFORM GASES Cambridge Press, Cambridge (1953)

Chatwin, P. C., "On the longitudinal dispersion of passive contaminant in oscillatory flows in tubes" J. Fluid Mech. 71 513 (1975)

Chen, N. H., Othmer, D. F., "New Generalized Equations for Gas Diffusion Coefficient", J. Chem. Eng. Data 7 37 (1962)

Crank, J., THE MATHEMATICS OF DIFFUSION 2nd ed, Clarendon Press, Oxford (1975)

Dreyer, G., Kahrig, E., Kirstein, J., Erpenbeck, J., Lange, Fr. "Grundlagen and Anwendungen einer neuen Diffusionsmethode in flüssiger Phase" Z. Naturforschung 23 498 (1968)

Edwards, D. K., Denny, V. E., Mills, A. F. TRANSFER PROCESSES AN INTRODUCTION TO DIFFUSION, CONVECTION, AND RADIATION 2nd Ed.; Hemisphere Publishing Corp., Washington D.C. (1979)

Fuller, E. N., Schettler, P. D., Giddings, J. C., "A New Method for Prediction of binary Gas-Phase Diffusion Coefficient", Ind. Eng. Chem. 58 (5) 19 (1966)

Harris, H. G., Goren, S. L. "Axial Diffusion in a Cylinder with Pulsed Flow" Chem Eng. Sci. 22 1571 (1967)

Hirschfelder, Joseph O., Bird, R. Byron, Spotz, Ellen L. "The Transport Properties of gases and Gaseous Mixtures" Chem. Revs. 44 205 (1949)

Jaeger, M. J., and Kalle, P., "Separation of gases by enhanced upstream diffusion" Sep. Sci. Technol. 27 691 (1992)

Jaeger, M. J., and Kurzweg, U. H., "Determination of the longitudinal dispersion coefficient in flows subjected to high frequency oscillations" Phys. Fluids 26 1380 (1983)

Jaeger, M. J., Soepardi, T., Maddanhian, A., and Kurzweg, U. H., "Diffusional separation of gases and solutes in Oscillatory flow" Sep. Sci. Technol. 26 503 (1991)

Johnston, Herrick L., McCloskey, Kenneth R. "Viscosities of Several Common Gases between 90°K. and Room Temperature" J. Phys. Chem. 44 1038 (1940)

Jones, Frank E., "Interpolation Formulas for Viscosity of Six Gases: Air, Nitrogen, Carbon Dioxide, Helium, Argon, and Oxygen", NBS TN 1186 (1984)

Joshi, C. H., Kamm, R. D., Drazen, J. M., Slutsky, A. S. "An Experimental Study of Gas Exchange in Laminar Oscillatory Flow" J. Fluid Mech. 133 245 (1983)

Jost, W. DIFFUSION IN SOLIDS, LIQUIDS, GASES 3rd Printing; Academic Press, New York (1960)

Kurzweg, U. H., "Enhanced Diffusional Separation in liquids by Sinusoidal Oscillation" Sep. Sci. Technol. 23 105 (1988)

Kurzweg, U. H., and Jaeger, M. J., "Tuning effect in enhanced gas dispersion under oscillatory conditions" Phys. Fluids 29 1324 (1986)

Kurzweg, U. H., and Jaeger, M. J., "Diffusional separation of gases by sinusoidal oscillations" Phys. Fluids 30 1023 (1987)

Kurzweg, U. H., Lindgren E. R., and Lothrop, B., "Onset of turbulence in oscillating flow at low Womersley number" Phys. Fluids A 1 1972 (1989)

Othmer, D. F., and Chen, H. T., "Correlating Diffusion Coefficients in Binary Gas Systems", Ind. Eng. Chem. Process Des. Dev. 1 249 (1962)

Perry, R. H., Chilton, C. H., CHEMICAL ENGINEER'S HANDBOOK McGraw-Hill Book Company, New York (1973)

Reid, R. C., and Sherwood, T. K., The Properties of Gases and Liquids, 2nd Ed. McGraw-Hill, New York (1966)

Schlichting, H. BOUNDARY LAYER THEORY McGraw-Hill, New York (1960)

Sharp, M. K., Kamm, R. D., Shapiro, A. H., Kimmel, E., Karniadakis, G. E., "Dispersion in a curved tube during oscillatory flow", J. Fluid Mech. 223 537 (1991)

Skelland, A. H. P. DIFFUSIONAL MASS TRANSFER John Wiley & Sons, New York (1974)

Taylor, G. I., "Dispersion of soluble matter in solvent flowing slowly through a tube" Proc. R. Soc. Lond. A 219 186 (1953)

Taylor, G. I., "Conditions under which dispersion of a solute in a stream of solvent can be used to determine molecular diffusion" Proc. Roy. Soc. A 225 473 (1954)

Watson, E. J., "Diffusion in oscillatory pipe flow" J. Fluid Mech. 133 233 (1983)

BIOGRAPHICAL SKETCH

Gregory Allen Zachrich was born May 10, 1955 in Defiance, Ohio, the second of five children. He attended the United States Merchant Marine Academy, graduating in 1977 with B.S. degrees in both marine engineering and naval transportation, and earning a Third Mate and Third Engineer license. During his 11-year career in the marine engineering field he ascended to the level of Senior Chief Engineer where he accepted delivery of two newly constructed ice-strengthened oil-product tankers. On his journeys he visited 93 countries and all seven continents, and has the distinction of being Chief Engineer on the largest ship ever to visit Antarctica. He acquired his masters degree in 1988 and his Ph.D. in 1995.

I certify that I have read this study and in my opinion it conforms to the acceptable standards of scholarly presentation and is fully adequate, in scope and quality, as a dissertation for the degree of Doctor of Philosophy.

Ulrich Kurzweg

Ulrich H. Kurzweg, Chairman
Professor of Aerospace Engineering,
Mechanics, and Engineering Science

I certify that I have read this study and in my opinion it conforms to the acceptable standards of scholarly presentation and is fully adequate, in scope and quality, as a dissertation for the degree of Doctor of Philosophy.

E. Rune Lindgren
Professor of Aerospace Engineering,
Mechanics, and Engineering Science

I certify that I have read this study and in my opinion it conforms to the acceptable standards of scholarly presentation and is fully adequate, in scope and quality, as a dissertation for the degree of Doctor of Philosophy.

Wei Shyy

Wei Shyy
Professor of Aerospace Engineering,
Mechanics, and Engineering Science

I certify that I have read this study and in my opinion it conforms to the acceptable standards of scholarly presentation and is fully adequate, in scope and quality, as a dissertation for the degree of Doctor of Philosophy.

Marc Jaeger

Marc Jaeger
Professor of Physiology

I certify that I have read this study and in my opinion it conforms to the acceptable standards of scholarly presentation and is fully adequate, in scope and quality, as a dissertation for the degree of Doctor of Philosophy.

William E. Lear, Jr.

William Lear
Assistant Professor of Mechanical Engineering

This dissertation was submitted to the Graduate Faculty of the College of Engineering and to the Graduate School and was accepted in partial fulfillment of the requirements for the degree of Doctor of Philosophy.

May 1995

Winfred M. Phillips
Dean, College of Engineering

Karen A. Holbrook
Dean, Graduate School